INVESTIGATING THE CAUSES OF A LANDSLIDE IN TERRA NATIVA SUBDIVISION AND DESIGNING SLOPE STABILIZATION USING RECYCLED PLASTIC PINS

by

Clara Klamm

A thesis

submitted in partial fulfillment

of the requirements for the degree of

Master of Science in Civil Engineering

Boise State University

August 2023

BOISE STATE UNIVERSITY GRADUATE COLLEGE

DEFENSE COMMITTEE AND FINAL READING APPROVALS

of the thesis submitted by

Clara Klamm

Thesis Title:	Investigating the Causes of a Landslide in Terra Nativa Subdivision and Designing Slope Stabilization Using Recycled Plastic Pins
Date of Final Oral Examination:	26 April 2023

The following individuals read and discussed the thesis submitted by student Clara Klamm, and they evaluated the student's presentation and response to questions during the final oral examination. They found that the student passed the final oral examination.

Bhaskar Chittoori, Ph.D., P.E.	Chair, Supervisory Committee
Seth Olsen, P.E.	Member, Supervisory Committee
Nick Hudyma, Ph.D., P.E.	Member, Supervisory Committee

The final reading approval of the thesis was granted by Bhaskar Chittoori, Ph.D., P.E., Chair of the Supervisory Committee. The thesis was approved by the Graduate College.

DEDICATION

To my parents Joni and Steve for their unfailing support.

ACKNOWLEDGMENTS

Many thanks to my committee members for their time and support in helping me accomplish this goal.

ABSTRACT

In early 2016, five homes along Alto Via Court in the Terra Nativa Subdivision of the Boise Foothills began to move. By May of 2016, the street was closed due to safety concerns, and a few years later, the homes were demolished. Despite the heartbreak and legal action that followed the event, a definitive cause of the landslide was never identified. To date, the site remains vacant. This research aims to investigate the potential causes of the slide to help identify the contributing factors that resulted in the mishap. In addition, the research seeks to design a way to stabilize the slope using recycled plastic pins (RPPs), which are durable, slender pins made from recycled materials that can reinforce a slope by driving the pins into the slope face to intercept the sliding surface. Results of the research found that surface runoff and irrigation were the greatest contributors to slope failure. Using average strength values of RPPs, a variety of reinforcement patterns were investigated. RPPs spaced at 3 feet in-plane and out-of-plane over the distance of the entire slope and RPPs spaced at 2 feet only at the slope crest and toe were both successful in bringing the slope factor of safety (FOS) to above 1.5. The 2-foot spacing is recommended due to having the least amount of reinforced area. Material costs to reinforce the entire area are estimated to be approximately 4 million dollars.

TABLE OF CONTENTS

LIST OF TABLES

LIST OF FIGURES

LIST OF PICTURES

LIST OF ABBREVIATIONS

AASHTO	American Association of State Highway and Transportation Officials
ACHD	Ada County Highway District
ASTM	American Society for Testing and Materials
FOS	Factor of Safety
ft/s	Feet Per Second
gpm	Gallons Per Minute
LEM	Limit Equilibrium Method
NDPES	National Pollutant Discharge Elimination System
pcf	Pounds Per Cubic Foot
PF	Probability of Failure
psf	Pounds Per Square Foot
RPP	Recycled Plastic Pin
TSF	Terteling Springs Formation

CHAPTER ONE: INTRODUCTION

In early 2016, five homes along Alto Via Court in the Terra Nativa Subdivision of Boise, Idaho began to move. The damage continued to worsen over the following months. By the beginning of May, Alto Via Court had been closed to the public (Shelton, 2016). By September, the damage was described as looking "like an earthquake" (McFarland, 2016). Homes fell apart, pavement cracked, and sidewalks buckled, as shown in Picture 1 (Idaho News, 2017).

Picture 1. Damage at Alto Via Court

Damage started with the Sericati residence at 289 Alto Via Court—see Picture 2—in January of 2016 with minor internal cracking. In the months that followed, the

damage worsened and spread to all other homes on the street, except for the home at 238 Alto Via Court, which was narrowly missed by the slide (Woodworth et al., 2016). By the beginning of May, the Ada County Highway District (ACHD) Commission had closed the entire street for safety reasons (Shelton, 2016). In 2018, five of the six original homes were demolished (KTVB, 2018).

Picture 2. Lots at Alto Via Court (Courtesy QGIS)

Due to a ground movement exemption, insurance would not cover the damage. This led to heartbreak and a slew of legal action, as homeowners were forced to move out while still paying their mortgages (Berg, 2016a). In April of 2018—after over two years of litigation—a settlement was finally reached that dismissed the previous lawsuits. The City of Boise paid the five homeowners $257,500 to be split between them. In addition, the City paid for the demolition of the homes and topsoil stabilization, which totaled $57,500. The purpose of the settlement was to protect taxpayers, and the City made sure

to state that it was not an admission of liability (KTVB, 2018). In 2019, the lots were auctioned, but no building permits were issued ("Foothills properties deemed uninhabitable after landslide are auctioned," 2019). To date, no definitive cause of the slide has been identified and the site remains vacant.

Stabilization of the site could prove costly (Berg, 2016b). However, an exciting solution exists that has the potential to cut costs while at the same time utilizing recycled materials (Khan et al., 2016). Recycled plastic pins (RPPs) are slender manufactured lumber composed of industrial waste (Chen et al., 2007). They have traditionally been used in applications where durability even in extreme environments is critical, such as outdoor furniture, fencing, docks, and boat launches ("10 common commercial recycled plastic lumber uses," 2018). Initial research in Missouri, Iowa, and Texas has shown that RPPs can successfully stabilize slopes by driving the pins into the face of the slopes in a similar fashion to soil nailing (Khan et al., 2016).

The purpose of this research was to accomplish two main objectives. The first was to perform a back-analysis to determine the likely soil conditions at the site at the time of failure. This included investigating changes in groundwater conditions that may have played a role in the failure, such as roof runoff and lot irrigation, leaking utilities, and stormwater infiltration from Table Rock Road to the east of the site (Woodworth et al., 2016). The back-analysis was carried out with the limit equilibrium method (LEM) using the computer software Slide2 by Rocscience and was based on site data gathered over the last few decades, including boring logs and inclinometer readings. Once an understanding was established of the conditions at the site at the time of failure, a solution could be proposed.

The second research objective was to design and optimize a system of RPPs that stabilizes the slope against further movement and permits structures to be built. This was also carried out using Slide2, and pins were modeled as piles. Design variables to optimize included layout of the RPPs—such as spacing and angle of placement in the slope—and dimensions of the RPPs—such as length and cross-sectional area (Loehr & Bowders, 2007; Loehr et al., 2000), as well as strength properties of the RPPs, which vary depending on composition and manufacturer (Chen et al., 2007).

Stabilizing the Terra Nativa slide with RPPs presents a win-win situation. Not only does it limit movement, improve safety, and open highly desirable Boise real estate for development, but it does so while implementing an exciting, cost-effective technology that utilizes recycled materials.

CHAPTER TWO: BACKGROUND AND LITERATURE

This chapter presents the background for the site, including the timeline of events associated with the slope failure, generalized site soil conditions, and potential causes of the slide. An introduction to recycled plastic pins (RPPs) as a slope stabilization alternative concludes the chapter.

Site Background

In 2003 and 2004, Strata performed a geotechnical evaluation for the site at Alto Via Court, including information collected from the late 1990s. In this evaluation, Strata pointed to the potential for slope instability, and they performed a slope stability analysis. Factors of safety (FOS) were determined to be above 1.5 (Howard et al., 2003). A FOS above 1.0 means the slope is stable, while a FOS below 1.0 means the slope is unstable or has failed (McCarthy, 2007, p. 669). A FOS exceeding 1.5 is considered safe for slopes with structures, while a FOS exceeding 1.3 is considered safe for slopes not supporting structures (American Association of State Highway and Transportation Officials [AASHTO], 2017, p. 11-19). These results led Strata to conclude that the "slopes [would] remain stable, provided surface and subsurface water [was] controlled in these areas" (Howard et al., 2003, p. 24).

In 2007, construction began, and in 2008, lots, roadways, and utilities were completed. In 2008, a utility trench in the roadway exhibited settlement, and in 2013, approximately 4 feet of backfill was excavated and replaced to repair the trench

(Woodworth et al., 2016). From 2008 to the beginning of 2016, no movement was reported (Eberhart, 2016).

In January 2016, cracking was observed inside the Sericati residence at 289 Alto Via Court. Movement in the other homes quickly followed. Strata performed another geotechnical evaluation of the site in April 2016 and pointed to changes in groundwater as a potential cause of the movement. No definitive cause for the changes in groundwater was identified (Woodworth et al., 2016).

In May 2016, Alto Via Court was closed to the public due to safety concerns (Shelton, 2016). It has not been reopened since.

Picture 3 shows what is known about the extent of the failure at the site with the black dotted line denoting the approximate location of the tension crack. The picture also shows the locations of the explorations performed from 2003 through 2021. Many of these were performed by Strata with additional field investigations by Cartwright Engineers and Innovate Geotechnical (IGEO).

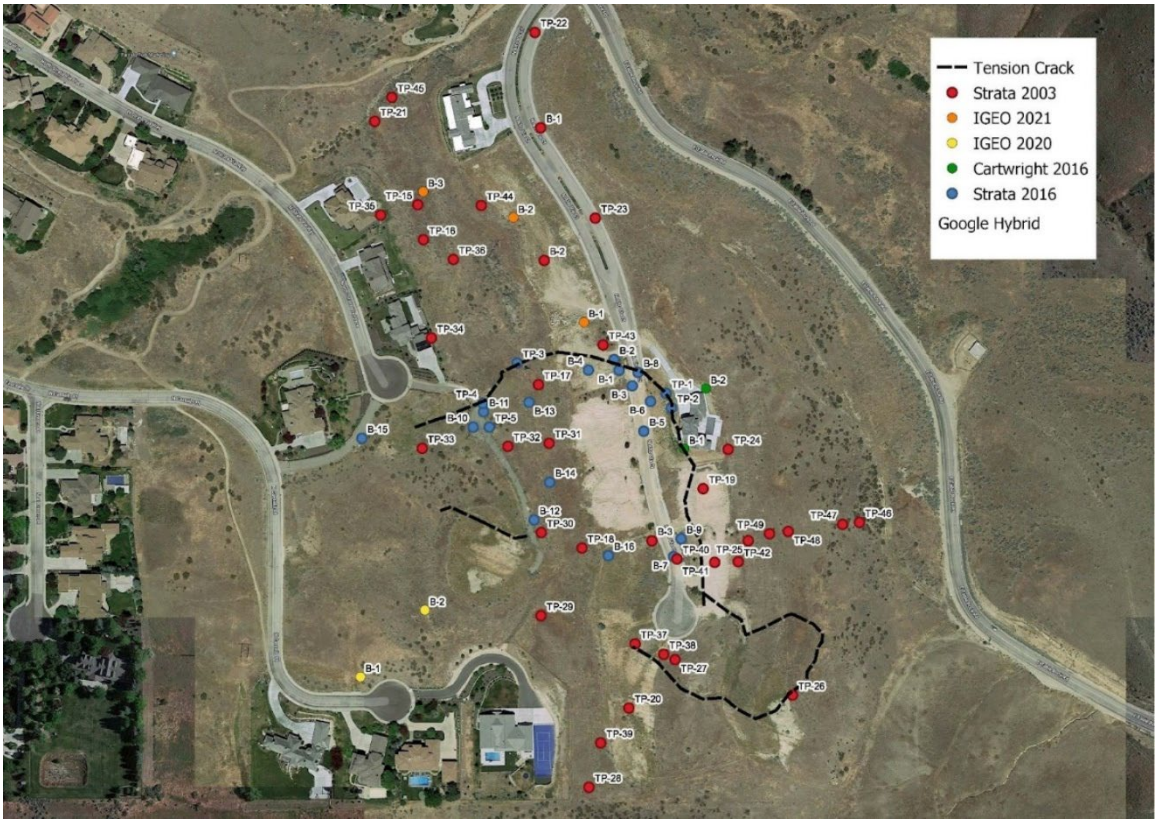

Picture 3. Extent of Failure and Exploration Locations (Courtesy QGIS)

An analysis of the explorations performed reveals that the subsurface profile consists primarily of six main soil types. In general, any structural fill placed on the site is followed by sandy clay to clayey sand. Underlying the clay is elastic silt, followed by indurated sand with silt and minor gravel and claystone (Howard et al., 2003; Olsen, 2016; Olsen & Klamm, 2020; Olsen & Klamm, 2021; Woodworth et al., 2016). This layer is referred to as the Terteling Springs Formation (TSF) and was often difficult to excavate (Howard et al., 2003). Inclinometer readings collected by Strata show that the failure plane occurs through the elastic silt layer at the interface with TSF (Woodworth et al., 2016). A rock outcropping at the center north region of the site consists primarily of a weathered basalt conglomerate and appears to restrict movement from occurring farther north (Olsen & Klamm, 2021).

Groundwater changes have frequently been cited as the primary cause of the movement at Alto Via Court, although no definitive cause for these changes has been identified. Strata pointed to four potential causes that require further investigation to confirm or refute (Woodworth et al., 2016).

The first potential cause for the changes in groundwater is surface runoff. This includes runoff water from the roofs of the homes and lawn irrigation. The second is leaking utilities. Although checking for leaking utilities was discussed, there is no evidence that this was ever carried out. Third, upgradient stormwater infiltration from Table Rock Road to the east of the site means water would enter the soil uphill of the failure and travel downslope (Woodworth et al., 2016). The reason this has frequently been cited as a potential cause of the movement is because ACHD performed roadway drainage work along Table Rock Road in the fall of 2015 that resulted in stormwater runoff discharging into the area immediately above and east of the site (Eberhart, 2016; Woodworth et al., 2016). Finally, changes in groundwater could simply be caused by natural groundwater fluctuations (Woodworth et al., 2016). Because of the infinite number of possibilities this last scenario includes, it was disregarded for the purposes of this research.

Groundwater is a problem for several reasons. One major reason is simply that water adds weight to the slide mass, making the soil heavier and causing it to move downslope. In addition, soil experiences apparent cohesion. When that soil becomes saturated, in essence it greases up the soil particles so that they slide past each other more easily, thus eliminating apparent cohesion and allowing the soil mass to slide downhill. An increase in water also means an increase in pore water pressure, thereby decreasing

effective stress and shear strength (Woodworth et al., 2016). If a sliding mass is initially dry, its effective stress is equal to the total stress, which in turn means that the shear strength is equal to the equation below, where τ_f is shear strength, c' is cohesion, σ is total stress, and φ' is the internal friction angle.

$$\tau_f = c' + \sigma \tan(\varphi')$$

If water is introduced, it increases the pore water pressure, causing the effective stress to decrease, where σ' is effective stress and u is pore water pressure.

$$\sigma' = \sigma - u$$

A decrease in the effective stress corresponds to a decrease in the shear strength.

$$\tau_f = c' + \sigma' \tan(\varphi') = c' + (\sigma - u) \tan(\varphi')$$

A lower shear strength means the soil mass will slide more easily.

An understanding of the conditions that led to failure is critical in order to recommend an appropriate stabilization alternative. A discussion of RPPs as a stabilization alternative is presented in the following section.

Introduction to Recycled Plastic Pins

Recycled plastic pins (RPPs) are slender plastic pins of varying length and cross section sometimes referred to as recycled plastic lumber. They are manufactured out of industrial wastes which consist primarily of polymeric materials, usually high- or low-density polyethylene. Varying amounts of sawdust, fly ash, and other byproducts are also added (Chen et al., 2007). An example of RPPs used in slope stability applications is given in Picture 4 (Ahmed, 2019).

Picture 4. Example of Recycled Plastic Pins

RPPs are manufactured using either compression molding or extrusion forming. The waste materials are pulverized, blended, and heated until slightly melted. With compression molding, the blend is then formed into molds of specific shape and size. With extrusion forming, the blend is forced through a die of desired cross section, allowing various lengths to be more easily manufactured (Chen et al., 2007).

Traditionally, recycled plastic lumber has been used in applications where durability even in extreme environments is necessary, such as outdoor furniture, fencing, docks, and boat launches. Exposure to temperature extremes and the elements is common ("10 common commercial recycled plastic lumber uses," 2018).

In slope stability applications, RPPs are driven into the slope face to intercept the sliding surface and prevent slope failure by providing additional resistance along the slip plane, as demonstrated in Picture 5 (Khan et al., 2016; Loehr & Bowders, 2007; Loehr et al., 2000).

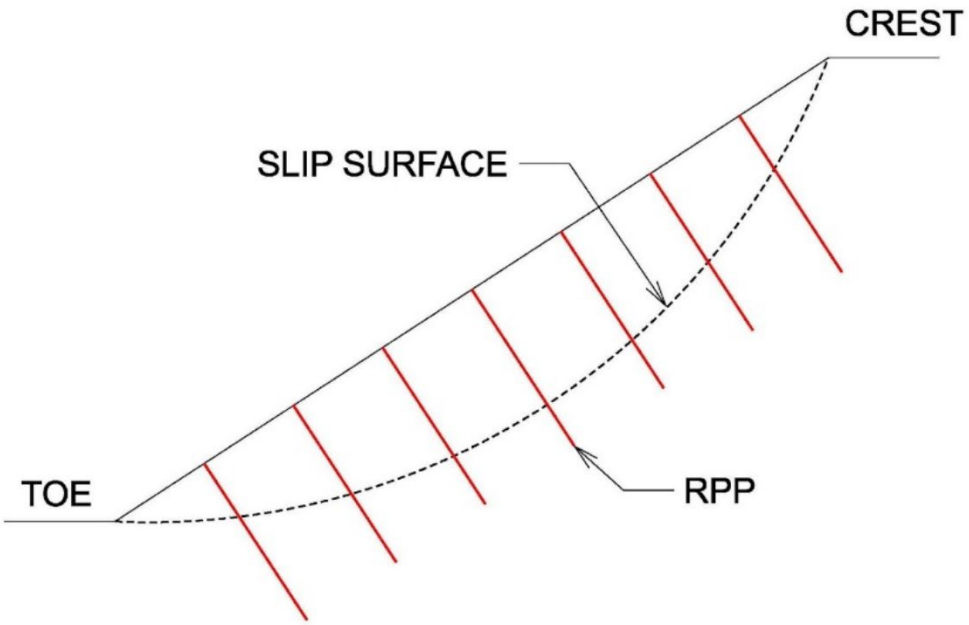

Picture 5. Basics of Recycled Plastic Pins

RPPs have been installed in slopes using several methods, including a backhoe-mounted hydraulic hammer, track-mounted hydraulic rig, track-mounted pneumatic rig, and drop-weight hammer rig (Loehr & Bowders, 2007). Khan et al. found that a crawler-type drilling rig with a mast-mounted vibratory hammer worked well for installation (2016). RPPs are installed either vertically or perpendicular to the slope face (Loehr & Bowders, 2007).

To design a system of RPPs, it is important to understand the potential modes of failure that can occur. After installation of the pins, the slope can fail because of pull out due to insufficient pin length, failure of the pins in shear or bending, or failure of the soil

between and around the pins. For this reason, designs that consider the depth of the sliding surface, pin capacity, and pin spacing are critical (Loehr et al., 2000).

The pin capacity can be difficult to determine. This is in part because manufacturers can change the blend of constituents in RPPs to obtain different engineering properties, leading to substantial variation in the properties of commercially available RPPs (Chen et al., 2007). Determination of the engineering properties is also highly dependent on the strain or deformation rate that is used while testing them. The ASTM standards use a higher strain rate than is likely to be experienced in the field, and using a higher strain rate tends to lead to a higher estimation of the strength properties. It is important that designers take this into consideration and determine the design strength using field strain rates and not the ASTM standards (Chen et al., 2007). Bowders et al. (2003) provide the prevailing engineering properties of RPPs from different manufacturers. The ASTM standards were followed in the determination of these properties except that the nominal strain rate was taken as one-fifth of the ASTM standard. For this reason, the results of Bowders et al.'s research were relied upon for this research.

A discussion of RPPs as a slope stabilization alternative would not be complete without a discussion of creep. Creep is a concern because plastic is more susceptible to bending creep than other materials like steel, concrete, and wood. Creep is by nature a long-term phenomenon, which makes it a challenging parameter to estimate within a reasonable timeframe. To speed things up, Loehr et al. (2000) tested RPP specimens at elevated temperatures, thus accelerating the time required to reach failure. Arrhenius modeling was then used to estimate the time required to reach failure at the site

temperature. The estimated time to failure due to creep was found to be 1000 years. In fact, this estimate is likely conservative because it was found using point loading. Distributed loading, which is more like the actual field conditions that the RPPs would experience, tends to fail even slower in creep, estimated at about 6000 years. Chen et al. (2007) also sought to estimate the creep behavior of RPPs in slope stability applications. Using tests at elevated temperatures and Arrhenius modeling, the authors found the estimated time to failure due to creep to be as little as three years. This is a drastically different estimate than Loehr et al. (2000). However, this is likely an underestimation. The RPPs that Chen et al. (2007) tested in the laboratory at room temperature did not show any cracks or signs of failure after five years. In addition, the time required to reach failure due to creep was estimated using point loading, and, as has been discussed, distributed loading results in a greater estimation of the required time to reach failure, and it is closer to the kind of loading RPPs would experience in the field. The authors conclude that failure in creep is not a concern, so long as the system of RPPs is designed properly (Chen et al., 2007).

RPPs are an attractive option for slope stabilization for several reasons. First, they are economical and cost-effective (Khan et al., 2016; Loehr et al., 2000). A preliminary economic comparison in Missouri showed that traditional rock armor is almost 1.5 times as expensive, and soil nailing is nearly five times as expensive (Loehr et al., 2000).

Because RPPs are made from recycled materials, they are environmentally attractive. The manufacture and use of RPPs reduce waste entering landfills and create a market for recycled plastics (Khan et al., 2016; Loehr & Bowders, 2007).

RPPs are less susceptible to degradation from biological and chemical sources than other stabilization alternatives (Khan et al., 2016; Loehr & Bowders, 2007). The fact that they are designed to be durable even outdoors in the elements makes them an attractive option in slope stabilization where they will be exposed to moisture and a range of temperatures ("10 common commercial recycled plastic lumber uses," 2018).

They are also lightweight, which lowers installation and transportation costs (Loehr & Bowders, 2007; see also Khan et al., 2016). However, their lightweight nature does not reduce performance. They have been found to be durable even in harsh driving conditions and environments. Furthermore, stability improvements were similar whether RPPs were used or steel reinforcement of the same size and spacing (Loehr et al., 2000).

Previous research on RPPs for slope stabilization shows that they have been successful in stabilizing surficial slope failures. A study of five Missouri slopes with a variety of conditions showed that slopes at the five sites had been stabilized for up to 6 years while control slopes had failed (Loehr & Bowders, 2007). Another Texas study used topographic surveys and instrumented RPPs with strain gages to monitor the performance of RPP-stabilized slopes. Results showed that the control sections had significantly greater settlement and higher strain readings, indicating that there was greater slope movement in the unreinforced zones compared to the reinforced zones (Khan et al., 2016).

However, more research is still needed to understand the capabilities of RPPs, especially as they relate to different slope geometries, soil conditions, and regions, as well as deep seated as opposed to surficial slope failures. This research seeks to do just

that. Experimental methods as they relate to performing the site back-analysis and stabilizing the slide with RPPs are discussed in the following chapter.

CHAPTER THREE: EXPERIMENTAL METHODS

This chapter presents the experimental methods of the research, including development of cross sections, selection of soil engineering properties, analysis of the various failure scenarios, and design of RPP reinforcement.

Five cross sections of the site at Alto Via Court were selected for analysis, as shown in Picture 6. The tension crack denoting the approximate extent of movement is also shown in the picture as the black dotted line.

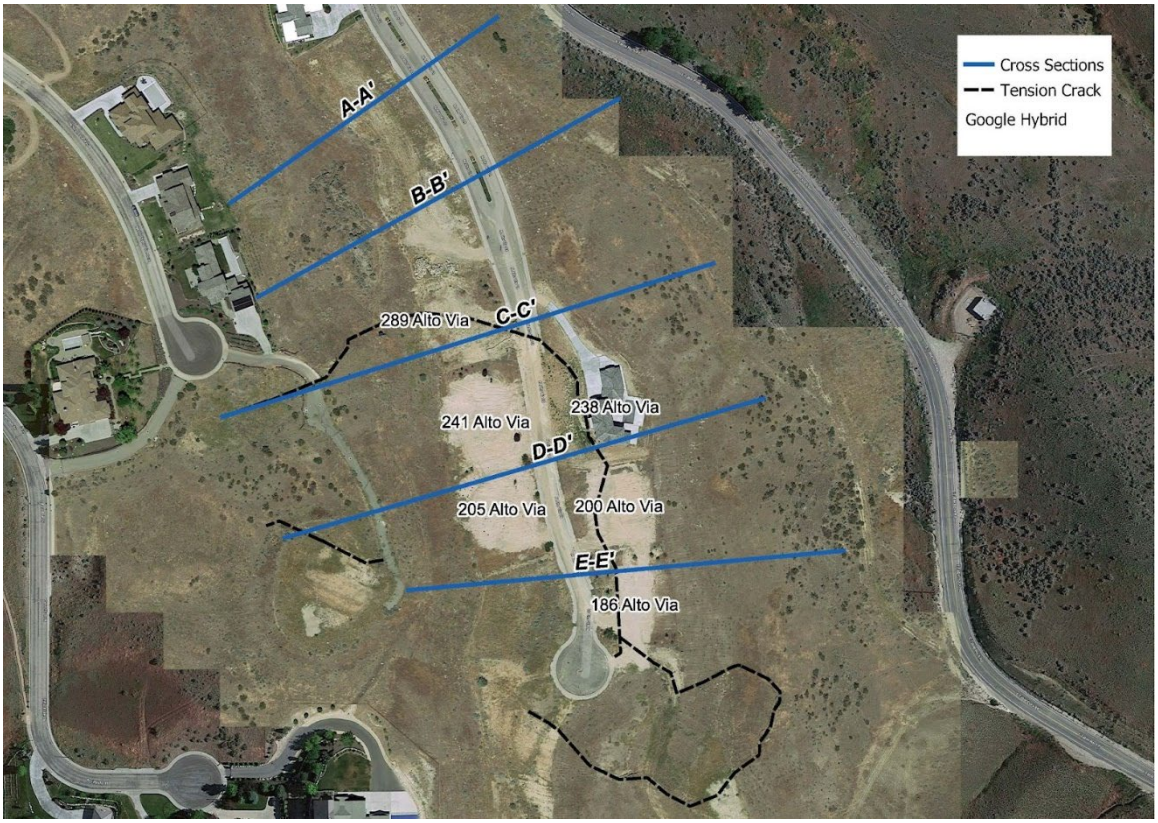

Picture 6. Cross Sections and Failure Area (Courtesy QGIS)

Failure began first at 289 Alto Via, or cross section C-C', before continuing south to cross sections D-D' and E-E'. For this reason, cross section C-C' was first focused on,

with the assumption that once it failed, movement would continue south. This is what was seen at the site. Movement at 289 Alto Via occurred in January 2016 and spread to the remaining homes—except for 238 Alto Via—in the months that followed (Woodworth et al., 2016). Cross sections A-A' and B-B' were unaffected, presumably because of the rock outcropping north and west of 289 Alto Via (Olsen & Klamm, 2021).

The cross sections were developed based on the subdivision grading plans (WHPacific, 2004). For each cross section, nearby explorations were selected to create the subsurface profile (Howard et al., 2003; Olsen, 2016; Olsen & Klamm, 2021; Woodworth et al., 2016). Soil properties were selected according to the Mohr-Coulomb failure criteria. Table 3.1 lists the soil types with their respective properties, as well as whether the properties are estimated or directly determined by lab testing.

Table 3.1 Soil Engineering Properties

Soil Type	**Cohesion (psf)**	**Friction Angle (degrees)**	**Unit Weight (pcf)**
Structural Fill	0 (estimated)	34 (estimated)	120 (estimated)
Sandy Clay (CL)	510 (lab testing)	21 (lab testing)	112 (lab testing)
Clayey Sand (SC)	512 (lab testing)	24 (lab testing)	115 (lab testing)
Elastic Silt (MH)	150 (lab testing)	20 (lab testing)	96 (lab testing)
Terteling Springs Formation (TSF)	130 (lab testing)	42 (lab testing)	125 (lab testing)
Rock Conglomerate	2000 (estimated)	36 (estimated)	135 (estimated)

The analyses were performed with Slide2 by Rocscience using the Bishop simplified, GLE/Morgenstern-Price, Janbu simplified, and Spencer methods. Using a

range of methods ensured that a thorough analysis was performed, and results could be relied upon. A brief discussion of variation between the methods is provided in Chapter 4.

The Slide2 analyses were performed using non-circular failure surfaces. In some instances, the depth of the failure surface was known from inclinometer readings collected by Strata. These failure surfaces appeared to follow a non-circular pattern as opposed to circular (Woodworth et al., 2016). In the case of a known failure surface, a Block Search was used, and the known path selected. Otherwise, the Cuckoo Search option was used.

The model implemented a probabilistic analysis using the Latin-Hypercube sampling method and Overall Slope analysis type. These methods were selected to provide a thorough analysis. The cohesion and friction angle of the upper layers—structural fill, CL, SC, and MH—were defined as random variables as part of the probabilistic analysis. Coefficients of variation were selected as 0.1 and 0.3 for the friction angle and cohesion, respectively, with a normal distribution (Ding & Loehr, 2019; Phoon & Kulhawy, 1999; Uzielli et al., 2006; Zevgolis et al., 2019; Zhang et al., 2010).

Pre-Failure

To perform the pre-failure analysis, a static water table was selected according to the water table information from the geotechnical reports (Howard et al., 2003; Olsen, 2016; Olsen & Klamm, 2021; Woodworth et al., 2016). The pre-failure analysis represents the period following 2008 before movement was reported. Lots and roadways

were completed in 2008, and the cross sections reflect that. However, homes had not been built and movement had not occurred.

Once the analyses for the pre-failure slopes were performed, the four failure scenarios were investigated, first individually, and then together. These include failure due to (1) loading from homes and failure due to changes in groundwater from (2) surface runoff and lot irrigation, (3) leaking utilities, and (4) upgradient stormwater infiltration from Table Rock Road (Woodworth et al., 2016). These scenarios are discussed in the following sections.

Loading from Homes

The effect of loading from homes was determined by applying a distributed load to the cross sections at the locations of the homes. The applied load from a two-story home was assumed to be 275 psf ("How much does a house weigh?", n.d.).

Groundwater Changes

All groundwater scenarios were modeled in Slide2 using a transient finite element groundwater seepage analysis. Results are highly dependent upon the saturated hydraulic conductivity of the soil, or K_S, which represents soil drainage (Han et al., 2012). Hence, a range of values for K_S were taken for each of the different soil layers and the analyses were performed for each. The minimum and maximum K_S values for each soil type are given in Table 3.2.

Table 3.2 Saturated Hydraulic Conductivity Values

Soil Type	**Minimum K_S (ft/s)**	**Maximum K_S (ft/s)**
Structural Fill	$3x10^{-5}$ (Kardena et al., 2014)	$3x10^{-3}$ (Kardena et al., 2014)
Sandy Clay (CL)	$3x10^{-8}$ (Kardena et al., 2014)	$3x10^{-6}$ (Kardena et al., 2014)
Elastic Silt (MH)	$3x10^{-8}$ (Kardena et al., 2014)	$3x10^{-6}$ (Kardena et al., 2014
Terteling Springs Formation (TSF)	$1x10^{-9}$ (Azam & Khan, 2013; da Rosa et al., 2013; Freeze & Cherry, 1979; Manna et al., 2019)	$1x10^{-5}$ (Azam & Khan, 2013; da Rosa et al., 2013; Freeze & Cherry, 1979; Manna et al., 2019)

Surface Runoff and Irrigation

Irrigation from lawns and surface runoff from roofs were modeled by combining precipitation data with assumed lawn watering rates. This combined infiltration rate was applied to each lot, starting in May of 2015, and continuing through the end of April of 2016.

Precipitation data was obtained from the National Pollutant Discharge Elimination System (NPDES) Phase II Annual Stormwater Monitoring Summary prepared for ACHD for water year 2019. The report contains precipitation data from two Boise locations for 2011 through 2019. The average precipitation values over the period from May of 2015 through April of 2016 are given in Table 3.3 (Brown and Caldwell, 2020, p. 37).

Table 3.3 Boise Precipitation Data

Time Period	Average Total Precipitation (inches)
May through June 2015	1.51
July through August 2015	1.12
September through October 2015	1.13
November 2015 through February 2016	5.12
March through April 2016	2.06

Lawn irrigation was assumed to start in mid-April at a rate of 1.5 inches per week and continue through the end of September (Smith, 2022). Surface runoff and irrigation were summed to obtain a total infiltration rate which was applied at the lot locations.

Leaking Utilities

Leaking utilities were mentioned as a potential cause of the slide; however, no concrete evidence shows that this occurred, nor does it indicate that it did not occur (Woodworth et al., 2016). Therefore, this analysis required some assumptions.

For the model, it was assumed that the water main under Alto Via Ct began leaking in January of 2016 and was never repaired, as there is no evidence of a repair taking place (Woodworth et al., 2016). The water main is an 8-inch diameter PVC pipe located in the street approximately 15 feet below the roadway surface (Treasure Valley Engineers, 2007a, 2007b). The assumption was made that pipe flow was as high as 1600 gallons per minute (Rowett, 2017). The maximum pipe flow was applied at the water main location from January 2016 when movement first occurred through April 2016.

Upgradient Stormwater Infiltration from Table Rock Road

In the fall of 2015, ACHD performed roadway drainage work along Table Rock Road that resulted in stormwater runoff discharging into the area immediately above and east of the site (Eberhart, 2016; Woodworth et al., 2016). Beyond that, no additional information is known regarding specific dates, the quantity of water, or the runoff area. Once again, assumptions had to be made.

The assumption was made that the drainage work took place starting September of 2015. Stormwater runoff volumes from two Boise locations are presented in the NPDES Phase II Annual Stormwater Monitoring Summary. The average stormwater runoff in cubic feet per acre for September 2015 through April 2016 are given in Table 3.4 (Brown and Caldwell, 2020, pp. 35-36).

Table 3.4 Boise Stormwater Runoff Data

Time Period	**Average Stormwater Runoff (cf/acre)**
September through October 2015	598
November 2015 through February 2016	4556
March through April 2016	2333

These quantities were converted to feet per day, which is Slide2's required input units for infiltration, by using Google Earth Pro to estimate that the runoff area is approximately 5 acres, and the infiltration area is approximately 500,000 square feet. These values are a rough estimate, but more precise details are unavailable.

Combined

Each of the three groundwater analyses were first performed separately to determine their individual effect before combining. Once the scenarios were combined,

the K_S values for the soil layers were varied to obtain a FOS equal to 1.0 at January of 2016, which is when failure first occurred. This best replicates the site conditions that are likely to have occurred. The results of the groundwater analyses are discussed in Chapter 4.

Stabilization with Recycled Plastic Pins

Recycled plastic pins (RPPs) were modeled in Slide2 as piles/micro piles. The critical design parameters to consider in the design of an RPP-stabilized slope are depth of the sliding surface, pin capacity, and pin spacing (Loehr et al., 2000). Pin length and angle of placement in slope are easily modeled by using the software to select the starting and ending point of each pin. Out-of-plane spacing of the support is specified when the pile/micro pile is defined.

For pin capacity, Slide2 requires shear strength in pounds as the input. The shear strength was calculated by first calculating the shear modulus (G) in psf, where E is Young's modulus or modulus of elasticity and v is Poisson's ratio.

$$G = \frac{E}{2(1+v)} = \frac{shear\ stress}{shear\ strain}$$

Shear stress was found by multiplying the shear modulus by shear strain. Shear strength in pounds was calculated by multiplying the shear stress by the cross-sectional area of the pin. Thus, Young's modulus, shear strain, Poisson's ratio, and cross-sectional area were all used as inputs. The values for these parameters are included in Table 3.5 along with the calculated shear strength. Bowders et al. (2003) provided Young's modulus at 1 percent strain and 5 percent strain. 1 percent strain was used in the calculations because specimens ruptured at 2 percent strain.

Table 3.5 Pin Capacity Parameters

Parameter	Minimum	Maximum	Average
Young's modulus at 1% strain (Bowders et al., 2003)	$1.11x10^7$ psf	$2.88x10^7$ psf	$1.85x10^7$ psf
Poisson's ratio (El-Bakary, 2008; Stowe et al., 2009)	0.32	0.49	0.42
Cross-sectional area (Bowders, et al., 2003; Khan et al., 2016)	3.5 in. x 3.5 in.	4 in. x 4 in.	3.5 in. x 3.5 in.
Shear strength	3,180 lbs	12,100 lbs	5,530 lbs

Since cross section C-C' is where failure started and it has the lowest FOS, RPP reinforcement was designed to bring the FOS at C-C' to above 1.5. Ten possible support layouts were analyzed, each for reinforcement installed both vertically and perpendicular to the slope face:

1. 6-foot by 6-foot square grid
2. 4-foot by 4-foot square grid
3. 3-foot by 3-foot square grid
4. 3-foot by 3-foot square grid at the crest and toe with 6-foot by 6-foot square grid at slope center
5. 2-foot by 2-foot square grid at the crest and toe with 6-foot by 6-foot square grid at slope center
6. 2-foot by 2-foot square grid at the crest and toe with 8-foot by 8-foot square grid at slope center

7. 2-foot by 2-foot square grid at the crest and toe with 10-foot by 10-foot square grid at slope center
8. 2-foot by 2-foot square grid at the crest and toe with 12-foot by 12-foot square grid at slope center
9. 2-foot by 2-foot square grid at the crest and toe with no reinforcement at slope center
10. 2.5-foot by 2.5-foot square grid at the crest and toe with no reinforcement at slope center

The FOS was calculated for each layout for a minimum, maximum, and average pile shear strength. Results are given and discussed in Chapter 4. A recommended layout is given in Chapter 4 and discussed in Chapter 5 along with a preliminary economic analysis. The recommended reinforcement pattern was modeled for the remaining cross sections and these results are given in Chapter 4.

CHAPTER FOUR: RESULTS AND DISCUSSION

This chapter presents the results of the research. This includes results of the back-analysis, including the investigation into individual and combined groundwater scenarios, and reinforcement patterns.

Results of Back-Analysis

When the pre-failure analyses were performed for each cross section, it was found that cross section C-C' had the lowest starting FOS. This is consistent with what was seen at the site; movement occurred first at cross section C-C', before moving south to D-D' and E-E' (Eberhart, 2016; Woodworth et al., 2016). Hence, the back-analysis was performed for cross section C-C' and results were applied to the remaining cross sections afterwards.

When loading from the homes was applied, it did not result in a FOS below 1, indicating that loading from the homes alone did not cause failure. Similarly, failure due to a leaking utility or stormwater infiltration from Table Rock Rd did not cause a decrease in the FOS. However, surface runoff from roofs and lawn irrigation did cause a significant decrease in the FOS, indicating that, according to this research, it had the greatest contribution towards failure of the slope. These numbers are reported for cross section C-C' in Table 4.1 below.

Table 4.1 Back-Analysis Results

Failure Scenario	FOS (mean)	PF (%)
Pre-Failure	1.314	0.9
Loading from Homes	1.291	1.3
Surface Runoff and Irrigation	0.907	82.9
Leaking Utility	1.314	0.9
Upgradient Stormwater Infiltration	1.314	0.9
Combined	0.926	76.9

Something to make note of here is how the FOS for surface runoff and irrigation is slightly lower than the combined FOS from all three scenarios. It is unclear why this would be the case. Intuitively, one would expect the combined FOS to be the lowest. This is likely just an anomaly in the computer program's calculations, as other small anomalies were also observed during the course of the research.

As part of the back-analysis, the K_S values of the individual soil layers had to be refined to determine the combination of K_S values that gave the "sweet spot" where failure occurred in January 2016. The final values are reported in Table 4.2. These values were used to model the remaining cross sections, along with a K_S equal to $3x10^{-6}$ ft/s for the clayey sand (Kardena et al., 2014) and $1x10^{-7}$ ft/s for the rock conglomerate (Freeze & Cherry, 1979; Manna et al., 2019).

Table 4.2 Final Saturated Hydraulic Conductivity Values

Soil Type	K_S (ft/s)
Structural Fill	$3x10^{-5}$
Sandy Clay (CL)	$3.5x10^{-7}$
Elastic Silt (MH)	$4x10^{-7}$
Terteling Springs Formation (TSF)	$1x10^{-9}$

As discussed in Chapter 3, the FOS was found using four methods: Bishop simplified, GLE/Morgenstern-Price, Janbu simplified, and Spencer. Figure 4.1 reports the values for each of these methods as they change over the course of the year from May 2015 through April 2016. The figure also presents the accompanying PF, which has an inverse relationship to the FOS.

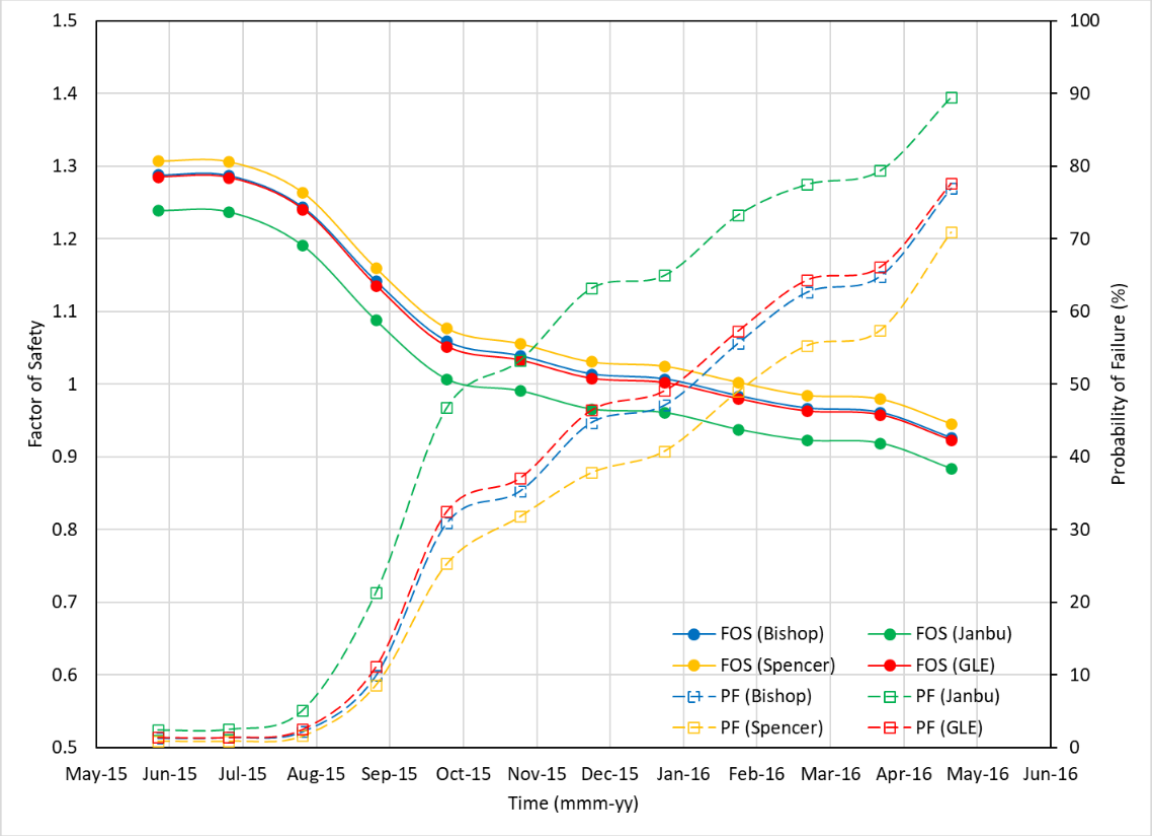

Figure 4.1 Change in Factor of Safety and Probability of Failure with Time

As can be seen from the figure, there is a reasonably close agreement between all four methods. Bishop and GLE/Morgenstern-Price have a very close agreement, while Spencer is slightly higher and Janbu is slightly lower. The level of agreement between the methods suggests a lack of modeling issues or problems resulting in erroneous data. In general, FOS and PF values reported in the graphs and tables of this document are for the Bishop simplified method.

Results of Recycled Plastic Pin Reinforcement

Once an understanding was reached of the site conditions resulting in failure, reinforcement with RPPs could be investigated. Ten reinforcement patterns were analyzed, each for orientations both vertical and perpendicular to the slope face, and for an average, minimum, and maximum shear strength of the RPPs. In all cases, RPPs were modeled to extend through the MH layer 1 foot into the dense TSF layer. The results are given in Table 4.3.

Table 4.3 Analysis of Reinforcement Layouts

Reinforcement Layout	Vertical/ Perpendicular	Average FOS	Minimum FOS	Maximum FOS
6'x6'	Vertical	1.035	0.993	1.257
	Perpendicular	1.048	0.992	1.249
4'x4'	Vertical	1.280	1.077	2.316
	Perpendicular	1.268	1.094	2.292
3'x3'	Vertical	1.782	1.282	-
	Perpendicular	1.775	1.274	-
3'x3' crest/toe, 6'x6' center	Vertical	1.249	1.066	2.154
	Perpendicular	1.242	1.083	2.138

Reinforcement Layout	Vertical/ Perpendicular	Average FOS	Minimum FOS	Maximum FOS
2'x2' crest/toe, 6'x6' center	Vertical	1.849	1.293	-
	Perpendicular	1.854	1.258	-
2'x2' crest/toe, 8'x8' center	Vertical	1.736	1.254	-
	Perpendicular	1.740	1.247	-
2'x2' crest/toe, 10'x10' center	Vertical	1.711	1.253	-
	Perpendicular	1.715	1.247	-
2'x2' crest/toe, 12'x12' center	Vertical	1.667	1.238	-
	Perpendicular	1.669	1.233	-
2'x2' crest/toe, None at center	Vertical	1.584	1.214	-
	Perpendicular	1.615	1.216	-
2.5'x2.5' crest/toe, none at center	Vertical	1.267	1.087	2.291
	Perpendicular	1.263	1.090	2.304

Reinforcement spaced at 6 feet, 4 feet, 3 feet, and a combination of 3 feet at the crest and toe and 6 feet at the center were analyzed first, based on the success of slopes previously stabilized with RPPs (Khan et al., 2016). As can be seen from the table, only the continuous 3-foot spacing resulted in an FOS that met or exceeded 1.5 for average strength RPPs. Reinforcement patterns with 2-foot spacing at the crest and toe and a variety of spacing distances at the center were then analyzed. All these configurations, including reinforcement at the crest and toe with no center reinforcement, resulted in acceptable FOS values for average strength RPPs. However, 2-½-foot spacing at the crest and toe with no center reinforcement was not sufficient. Hence, the two most economical reinforcement patterns that provided an acceptable FOS were the continuous 3-foot

spacing and the 2-foot spacing at the crest and toe with no center reinforcement. 2-foot spacing at the crest and toe with no center reinforcement is recommended due to having the smallest area that requires reinforcement.

As has been mentioned and can be seen from Table 4.3, all spacing patterns were analyzed for RPPs installed both vertically and perpendicular to the slope face. Figure 4.2 gives the change in FOS and PF for different continuous reinforcement spacing distances. The graph reports the FOS for average, minimum, and maximum RPP strengths, as well as the PF for the average RPP strength. In particular, however, the graph shows these values for RPPs installed both vertically and perpendicular to the slope face, with vertical reported in blue and perpendicular reported in red. There is extremely close agreement between the two angles of placement. Essentially, it makes no significant difference in the final stability whether RPPs are installed vertically or perpendicular to the slope face.

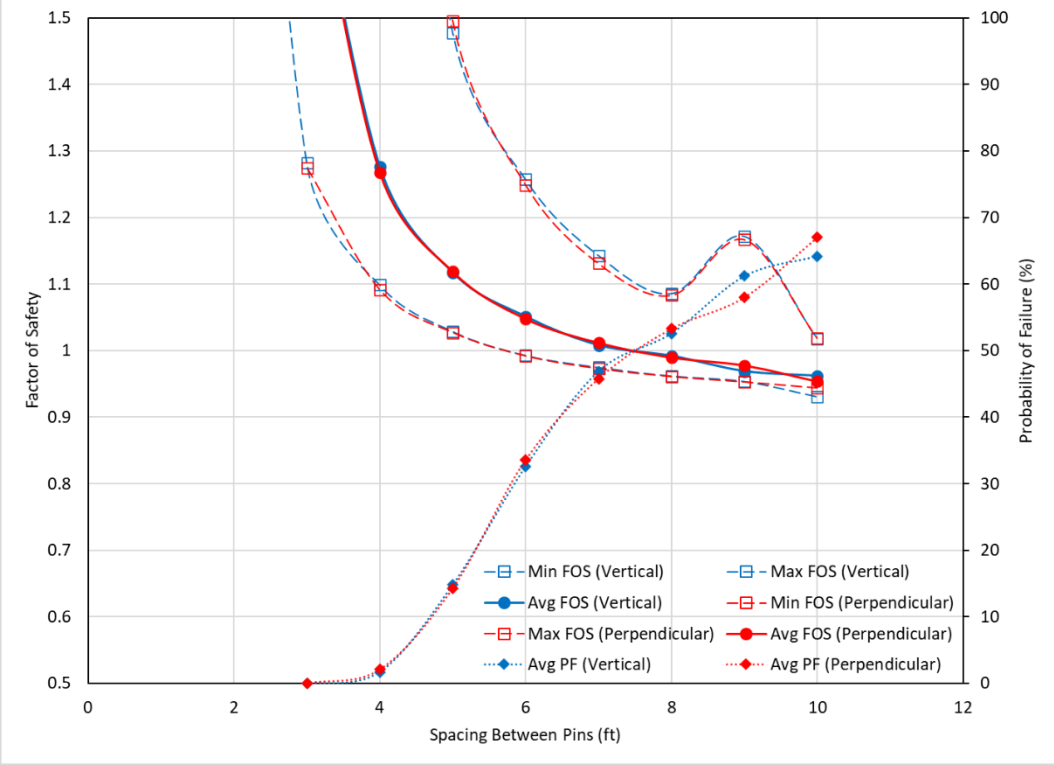

Figure 4.2 Change in Factor of Safety and Probability of Failure with Pin Spacing

Note that there is an increase in the FOS at the 9-foot pin spacing, resulting in a bump in the graph. It is unclear why this would be the case, as the increased FOS occurred only for the maximum strength RPPs. Most likely this is an anomaly in the computer program's calculations. As has been discussed, an anomaly was also observed with the FOS of the combined groundwater scenarios versus the FOS for surface runoff and irrigation only. Overall, the computer program was found to provide reliable, accurate data that fall within expectations; these slight anomalies are not considered to be a detriment to the research or an invalidation of the results.

Once the back-analysis was performed and the recommended reinforcement pattern determined for cross section C-C', the results were applied to the remaining cross sections. Cross sections A-A' and B-B' both had the same FOS before and after failure occurred. Neither cross section ever had a FOS that fell below 1.5, and no movement in the area north of the rock outcropping has been reported (Olsen & Klamm, 2021; Woodworth et al., 2016). This is most likely due to the rock outcropping, stronger soils overall in this area, and the fact that homes were never built there, so no surface runoff from roofs and lot irrigation ever occurred. For these reasons, this research does not consider reinforcement of the area north of the rock outcropping to be necessary. This area, in the opinion of this research, can support houses, given the natural strength of the soils and high FOS values for cross sections A-A' and B-B', combined with best building practices, adequate site drainage, and preferably xeriscaping that uses little to no water.

For the remaining cross sections—C-C', D-D', and E-E'—reinforcement with RPPs is recommended, using 2-foot spacing at the crest and toe that extends 1 foot into the dense TSF layer. Cross sections D-D' and E-E' were analyzed for this reinforcement

pattern. Results for all five cross sections showing the FOS before and after failure and following the installation of reinforcement are given in Table 4.4.

Table 4.4 Summary of Results

Cross Section	FOS Before Failure	FOS After Failure	FOS After Reinforcement
A-A’	1.629	1.629	N/A
B-B’	2.276	2.276	N/A
C-C’	1.314	0.926	1.584
D-D’	1.791	1.632	2.569
E-E’	3.252	3.009	4.874

CHAPTER FIVE: CONCLUSION

This research had two objectives, to determine the site conditions at the time of the failure of the slope and provide a recommendation for reinforcement with RPPs. Going into the research it was known that groundwater likely played a role in the failure (Woodworth et al., 2016), and that RPPs have successfully stabilized slopes in the past and are both an environmentally friendly and economical approach (Loehr et al., 2000; Loehr & Bowders, 2007; Khan et al., 2016).

An analysis of four modes of failure including loading from homes and three groundwater scenarios—surface runoff and irrigation, leaking utility, and stormwater infiltration—revealed that, according to this research, surface runoff and irrigation played the largest part in leading to failure. Table 5.1 presents the FOS for each of these potential modes of failure and the percent decrease in FOS from the original pre-failure value. As can be seen, leaking utility and stormwater infiltration did not affect the FOS, loading from homes resulted in an approximately 2 percent decrease in FOS, and surface runoff and irrigation contributed by far the largest decrease in FOS at approximately 31 percent.

Table 5.1 Cause(s) of the Slide

Failure Scenario	FOS	Decrease in FOS (%)
Pre-Failure	1.314	-
Loading from Homes	1.291	1.8
Surface Runoff & Irrigation	0.907	31.0
Leaking Utility	1.314	0.0
Stormwater Infiltration	1.314	0.0

As discussed in Chapters 3 and 4, ten patterns for RPP reinforcement were analyzed. For each pattern, RPP reinforcement installed vertically as well as perpendicular to the slope face were considered. In the end, reinforcement with 2-foot in-plane and out-of-plane spacing at the crest and toe that extends 1 foot into the dense TSF layer is recommended. There was little to no difference in performance between vertical and perpendicular reinforcement, although for this research the remaining cross sections were modeled using vertical reinforcement.

For the area north of the rock outcropping which includes cross sections A-A' and B-B', reinforcement is not considered necessary due to the rock and stronger native soils. For the remaining cross sections, the increase in FOS after reinforcement is given in Table 5.2. As can be seen, the reinforcement provides a minimum 57.4 percent increase across the slope.

Table 5.2 Increase in Factor of Safety with Reinforcement

Cross Section	FOS Before Reinforcement	FOS After Reinforcement	Percent Increase
C-C’	0.926	1.584	71.1
D-D’	1.632	2.569	57.4
E-E’	3.009	4.874	62.0

Table 5.3 presents an analysis of the recommended reinforcement and approximate cost. Out of the two acceptable reinforcement patterns that give an FOS of at least 1.5, a 2-foot spacing at the crest and toe covers the least amount of area. This configuration includes 44 rows of pins at the crest of the slope and 16 rows of pins at the toe. As discussed, reinforcing the area north of the rock outcropping is deemed unnecessary. The remaining area requiring reinforcement extends approximately 1000 feet south of the rock outcropping, meaning approximately 30,000 pins total would be required. Loehr and Bowders (2007) reported the cost of an 8-foot long RPP to be approximately $20 to $25, or an average of approximately $2.80 per linear foot.

The length of the pins required for RPPs installed vertically ranges from 5.5 ft to 83.5 ft. The weighted average length required for the crest, center, and toe were found to be 54.2 ft, 54.5 ft, and 27.3 ft, respectively. Assuming the price per linear foot holds at longer lengths, the approximate cost of each of the reinforcement layouts listed in Table 5.3 is shown.

Table 5.3 Reinforcement Layouts and Approximate Cost

Reinforcement Layout	Approximate # Pins	Approximate Cost ($)	Performance
6'x6'	6,700	0.95 million	Not Satisfactory
4'x4'	15,100	2.15 million	Not Satisfactory
3'x3' crest/toe, 6'x6' center	16,700	2.27 million	Not Satisfactory
3'x3'	26,900	3.82 million	Satisfactory
2'x2' crest/toe, none at center	30,000	3.95 million	Satisfactory

This research supports the idea that RPP reinforcement can be designed to stabilize the 2016 Terra Nativa slide in Boise and provides a recommended system of RPPs that accomplishes this by increasing the minimum FOS to above 1.5.

REFERENCES

10 common commercial recycled plastic lumber uses (2018, June 1). In *Tangent Materials*.

Ahmed, A. (2019, October 23). Sustainable slope stabilization using recycled plastic pin. *New York State Department of Transportation*. https://www.dot.ny.gov/divisions/engineering/structures/repository/events-news/2019_LBC_session_4-1.pdf

American Association of State Highway and Transportation Officials (2017). *AASHTO LRFD Bridge Design Specifications* (8th ed.).

Azam, S., & Khan, F. (2013, May). Geohydrological properties of selected badland sediments in Saskatchewan, Canada. *Bulletin of Engineering Geology and the Environment, 73*(2), 389-399.

Berg, S. (2016a, June 24). Boise Foothills homeowners: Many to blame for sliding houses. In *Idaho Statesman*.

Berg, S. (2016b, May 14). Owners of sliding Foothills homes prepare for legal battle. In *Idaho Statesman*.

Bowders, J. J., Loehr, J. E., Salim, H., Chen, C. (2003, January). Engineering properties of recycled plastic pins for use in slope stabilization. *Transportation Research Record*, *1849*(1849), 39-46. https://doi.org/10.3141/1849-05

Brown and Caldwell. (2020, January 3). NPDES Phase II: Annual Stormwater Monitoring Summary.

Chen, C., Salim, H., Bowders, J. J., Loehr, J. E., & Owen, J. (2007, February). Creep behavior of recycled plastic lumber in slope stabilization applications.

da Rosa, M., Agouridis, C. T., Warner, R. C. (2013, March). Potential use of weathered sandstone to construct a low permeability barrier to isolate problematic coal mine spoils. *Journal American Society of Mining and Reclamation, 2*(1), 49-67.

Ding, D., & Loehr, J. E. (2019). Variability and bias in undrained shear strength from different sampling and testing methods. *Journal of Geotechnical and Geoenvironmental Engineering*, *145*(10).

Eberhart, D. R. (2016, May 31). 3rd Party Review Preliminary Progress Report.

El-Bakary, M. A. (2008, April). Determining the opto-mechanical and geometrical properties of high-density polyethylene fibres. *Optics and Lasers in Engineering*, *46*(4), 328-335. https://doi.org/10.1016/j.optlaseng.2007.11.007

Freeze, A. R., & Cherry, J. A. (1979). *Groundwater* (pp. 26-30). : Prentice-Hall, Inc.

Foothills properties deemed uninhabitable after landslide are auctioned (2019, August 2). In *Idaho News*.

Han, J., Xie, J., Zhang, Y. (2012, May 25). Potential role of feldspathic sandstone as a natural water retaining agent in Mu Us sandy land, northwest China. *Chinese Geographical Science*, *22*(5), 550-555.

Howard, H. R., Comstock, C. M., & Howard, T. R. (2003, November 13). Geotechnical Engineering Evaluation: Proposed Nativa Terra Subdivision No. 3.

How much does a house weigh? (n.d.). *Survival Tech Shop*. https://www.survivaltechshop.com/how-much-does-a-house-weigh/

Idaho News. (2017). Sliding homes in the Boise foothills aren't holding up in winter. *Idaho News*. https://idahonews.com/news/local/sliding-homes-in-the-boise-foothills-arent-holding-up-in-winter-2017

Kardena, E., Helmy, Q., Funamizu, N. (2014). *Biosurfactants and Soil Bioremediation* (pp. 327-360). Research Gate.

Khan, M. S., Hossain, S., & Kibria, G. (2016, June). Slope stabilization using recycled plastic pins. *Journal of Performance of Constructed Facilities*, *30*(3), 1-10. doi:10.1061/(ASCE)CF.1943-5509.0000809

KTVB (2018, April 27). Documents reveal details of settlement between Boise, Alto Via homeowners. In *KTVB*.

Loehr, J. E., Bowders, J. J., & Salim, H. (2000, July). *Slope stabilization using recycled plastic pins - constructability*. University of Missouri - Columbia.

Loehr, J. E., & Bowders, J. J. (2007). *Slope stabilization using recycled plastic pins - phase III*. University of Missouri - Columbia.

Manna, F., Murray, S., Abbey, D., Martin, P., Cherry, J., Parker, B. (2019, April 30). Spatial and temporal variability of groundwater recharge in a sandstone aquifer in a semiarid region. *Hydrology and Earth System Sciences, 23*, 2187-2205.

McCarthy, D. F. (2007). *Essentials of Soil Mechanics and Foundations: Basic Geotechnics* (7th ed.). : Pearson Prentice Hall.

McFarland, K. (2016, September 6). Damage to homes in Boise foothills continues: 'It looks like an earthquake.' In *WTOV.*

Olsen, S. P. (2016, October 26). Geotechnical Soils Report: 238 Alto Via Residence.

Olsen, S. P., & Klamm, C. (2020, July 3). Geotechnical Engineering Report: 118 N Castello Pl.

Olsen, S. P., & Klamm C. (2021, June 29). Geotechnical Engineering Report: 403 N Alto Via Court.

Phoon, K., & Kulhawy, F. H. (1999, August). Characterization of geotechnical variability. *Canadian Geotechnical Journal*, *36*(4), 612-624.

Rowett, A. (2017, November 14). From hoselines to hydrants: Understanding water supply. *Firehouse*. https://www.firehouse.com/operations-training/hoselines-water-appliances/article/12373752/water-supply-for-fireground-operations-hydrants-ldh-water-main-firefighter-training

Shelton, B. (2016, May 5). Landslide risk leads to road closures near Table Rock. In *KTVB.*

Smith, M. (2022, January 16). 10 spring lawn care tips for Boise. *Lawn Love*. https://lawnlove.com/blog/spring-lawn-care-tips-boise/

Stowe, J. Q., Predecki, P. K., Laz, P. J., Burks, B. M., Kumosa, M. (2009, July). Probabilistic molecular dynamics evaluation of the stress-strain behavior of polyethylene. *Acta Materialia*, *57*(12), 3615-3622. https://doi.org/10.1016/j.actamat.2009.04.023

Treasure Valley Engineers (2007a, February 21). Nativa Terra Subdivision No. 3 Phase 2: E. Alto Via Place Plan & Profile.

Treasure Valley Engineers (2007b, February 21). Nativa Terra Subdivision No. 3 Phase 2: United Water Plan.

Uzielli, M., Lacasse, S., Nadim, F., Phoon, K. (2006, December). Soil variability analysis for geotechnical practice. 1-103.

WHPacific. (2004, October 18). Nativa Terra Subdivision No. 3: Grading Control Plan.

Woodworth, M. G., Miller, S. M., & Gado, D. P. (2016, April 15). Geotechnical Consulting Services: Phase 1 Summary Report Terra Nativa Subdivision.

Zevgolis, I. E., Koukouzas, N. C., Roumpos, C., Deliveris, A. V., Marshall, A. M. (2019, June). Evaluation of geotechnical property variability: The case of spoil material from surface lignite mines. *Safe Kozani*, 236-245.

Zhang, J., Tang, W. H., Zhang, L. M. (2010, January). Efficient probabilistic back-analysis of slope stability model parameters. *Journal of Geotechnical and Geoenvironmental Engineering*, *136*(1), 99-109.

APPENDIX A

Results of Slope Stability Analysis Before Failure

The following pages present the five cross sections with their accompanying factors of safety for the pre-failure analysis.

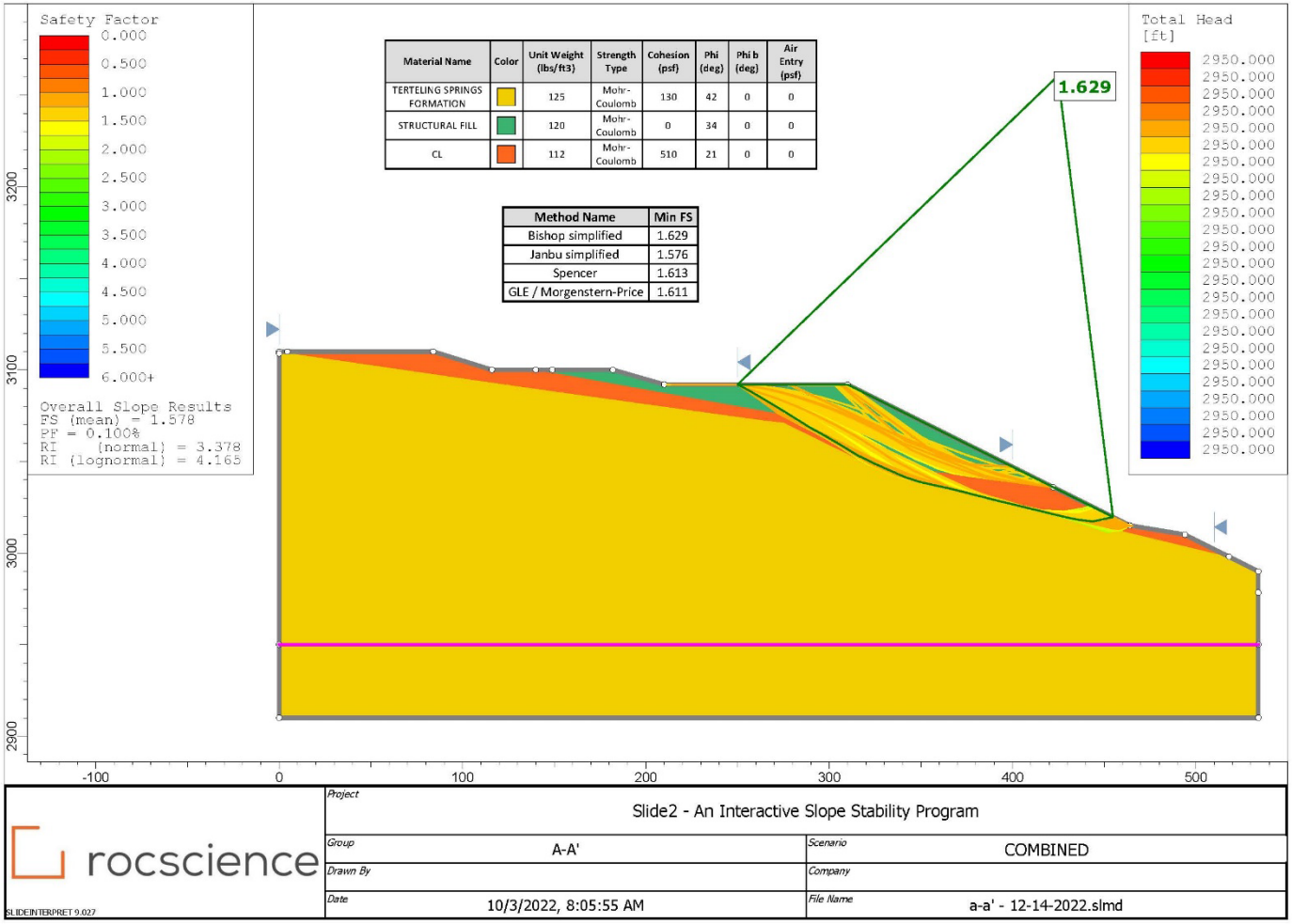

Figure A.1 Cross Section A-A' Before Failure

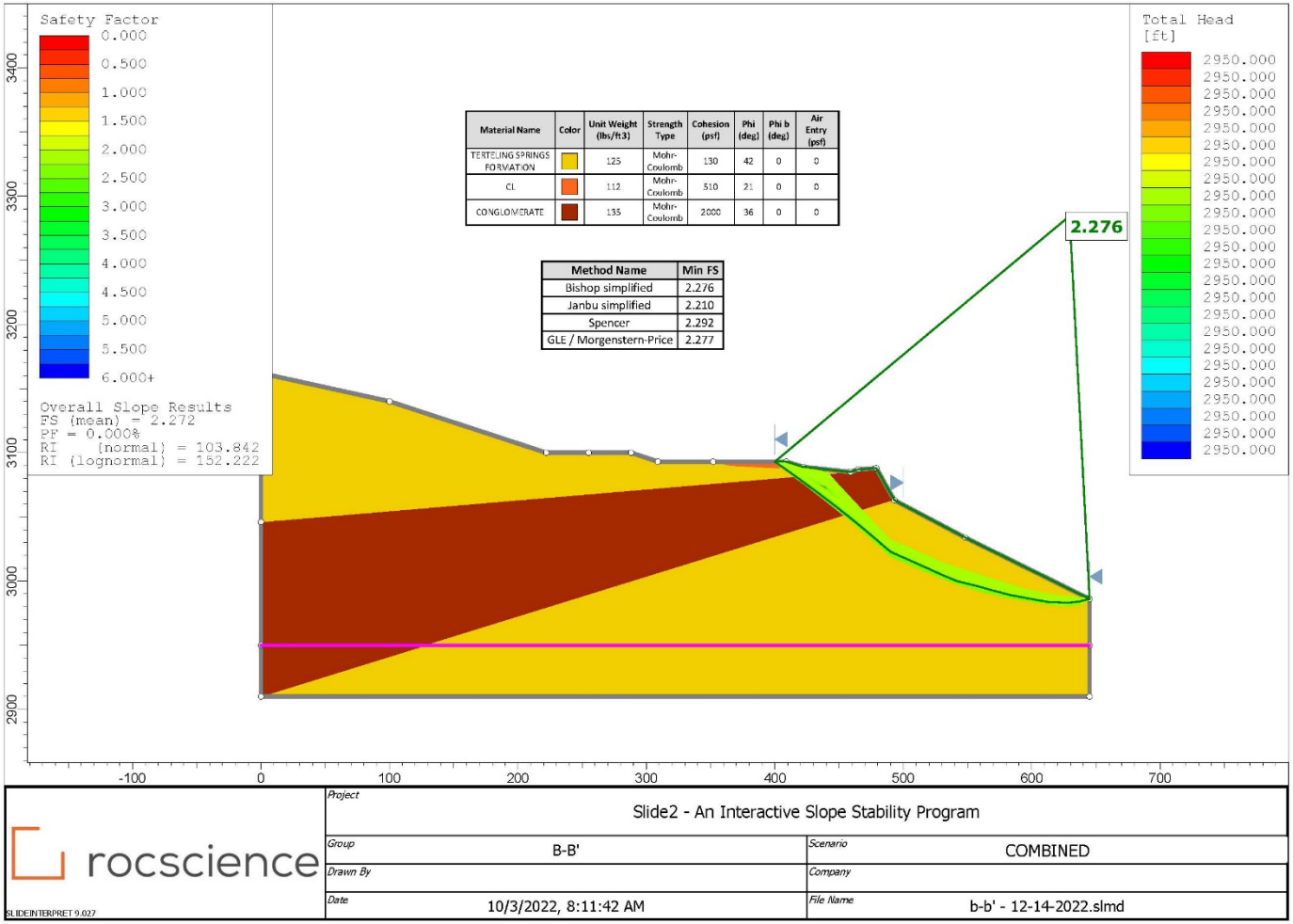

Figure A.2 Cross Section B-B' Before Failure

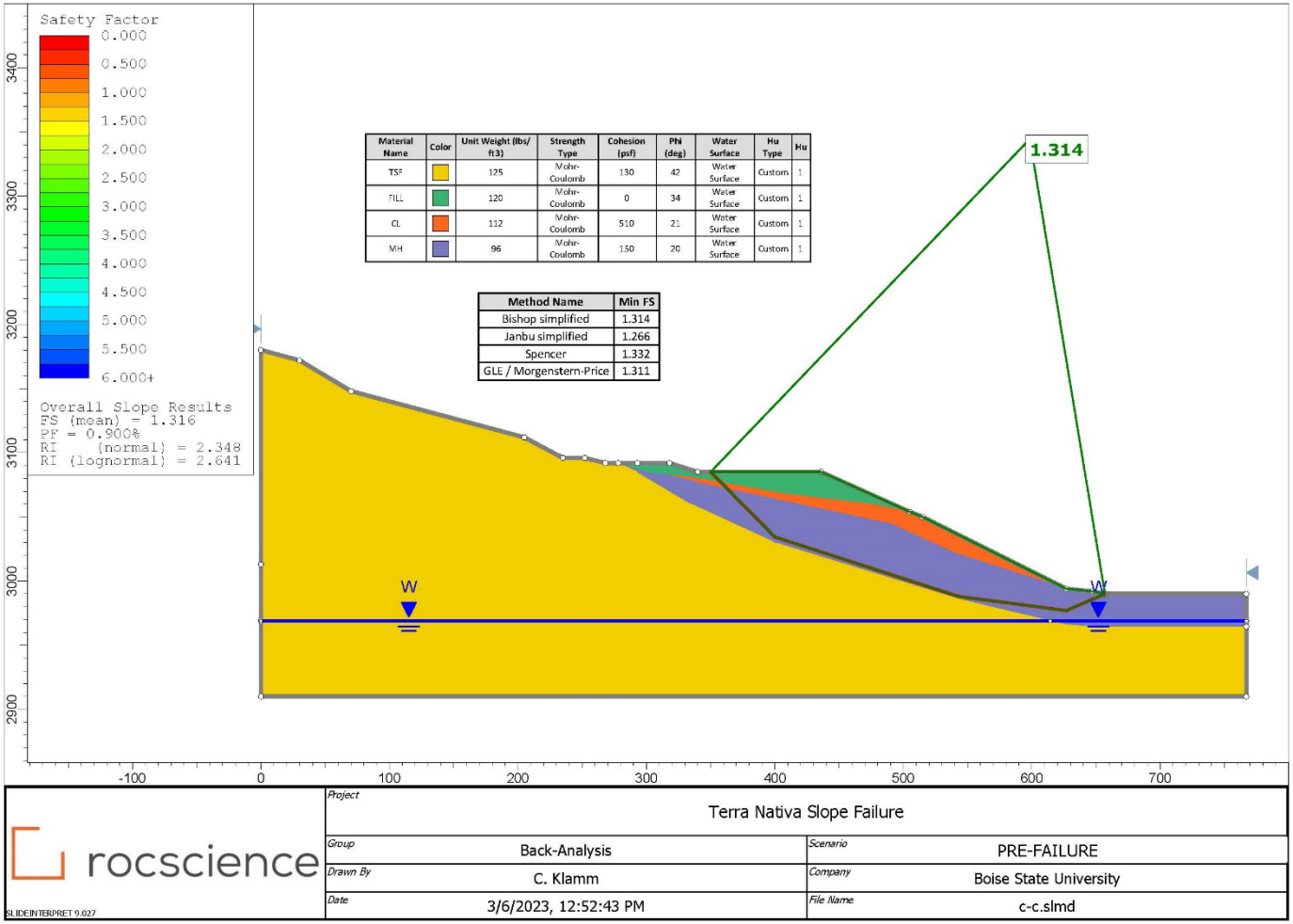

Figure A.3 Cross Section C-C' Before Failure

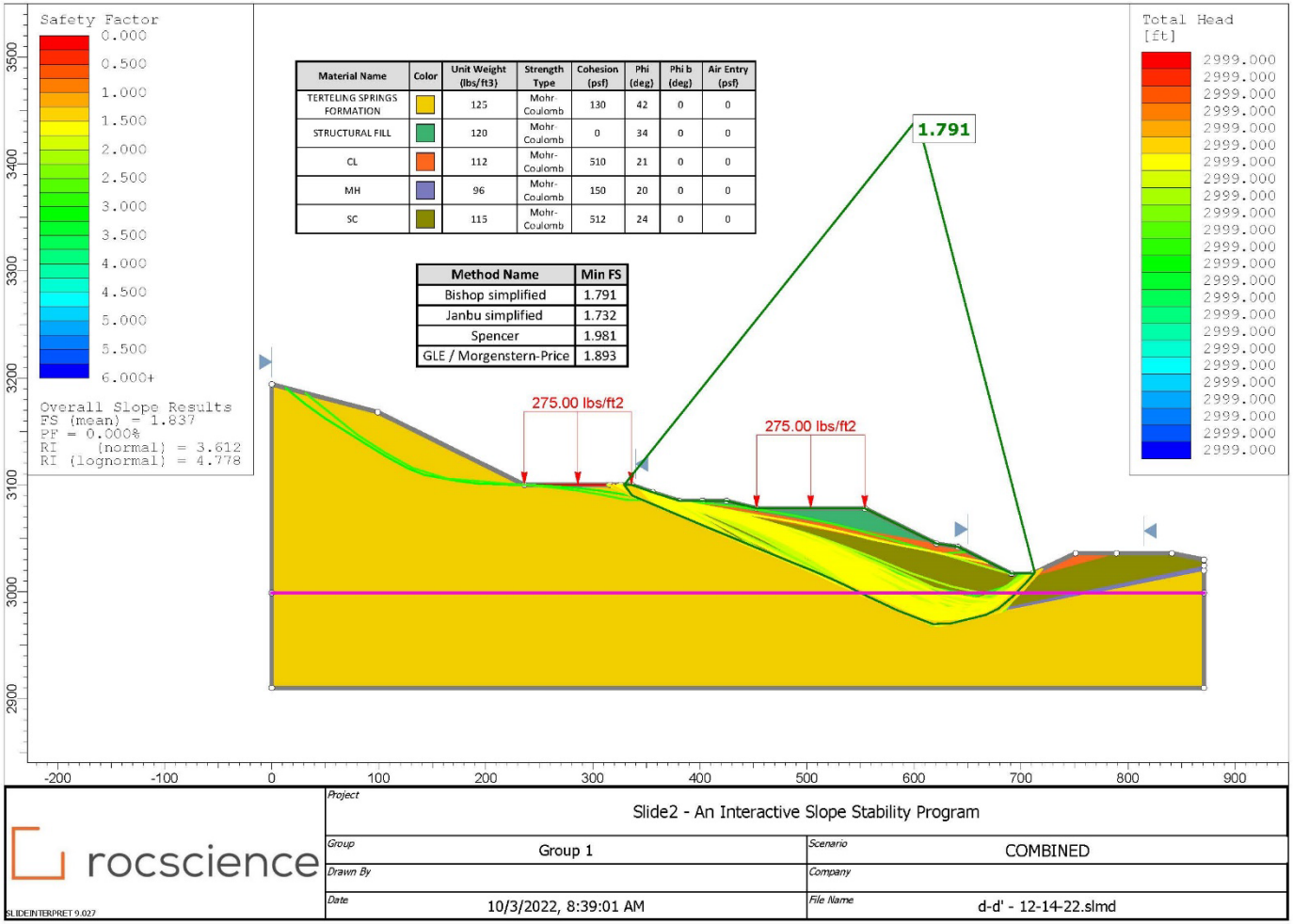

Figure A.4 Cross Section D-D' Before Failure

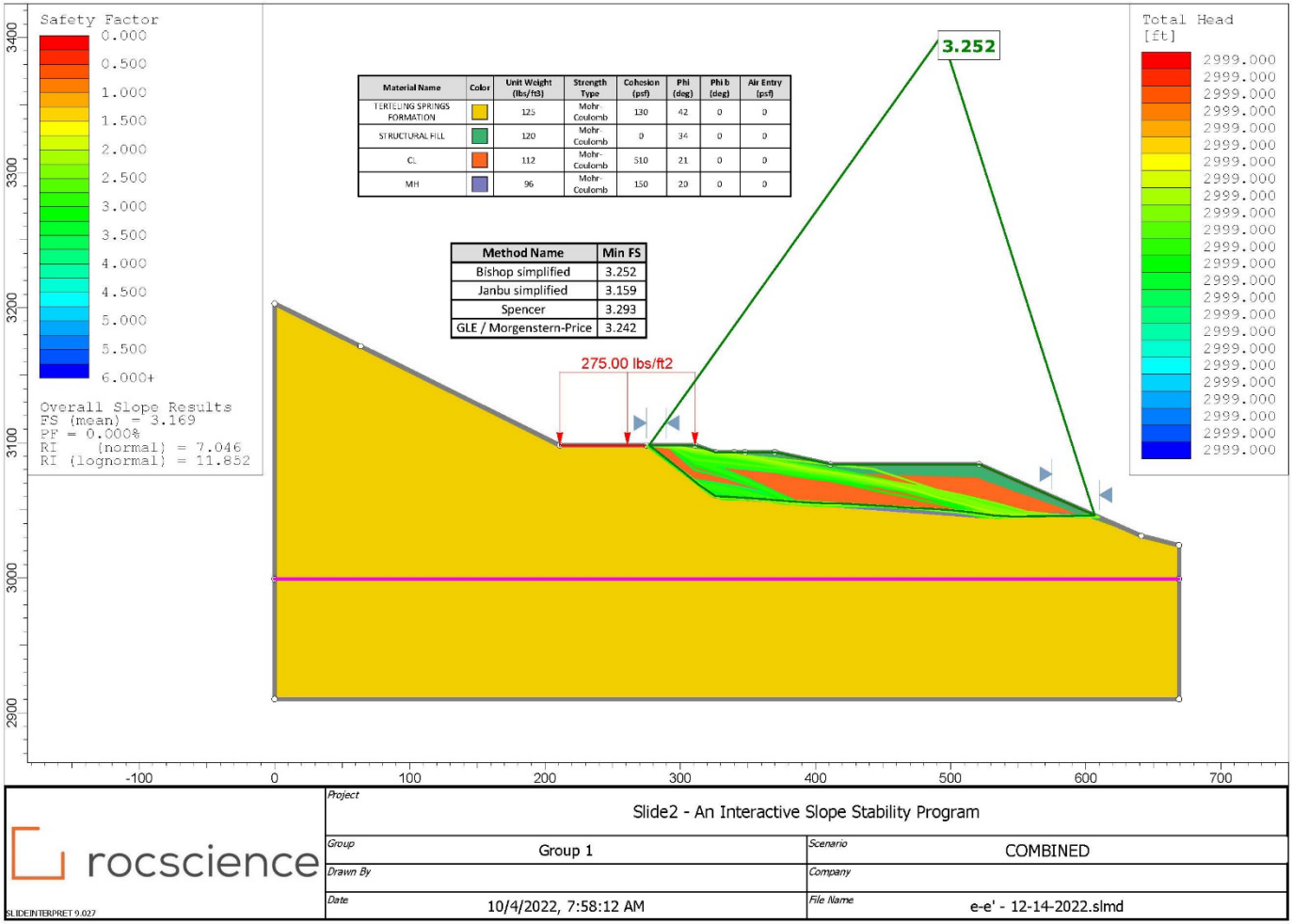

Figure A.5 Cross Section E-E' Before Failure

APPENDIX B

Results of Slope Stability Analysis After Failure

The following pages present the five cross sections with their accompanying factors of safety for the combined post-failure analysis.

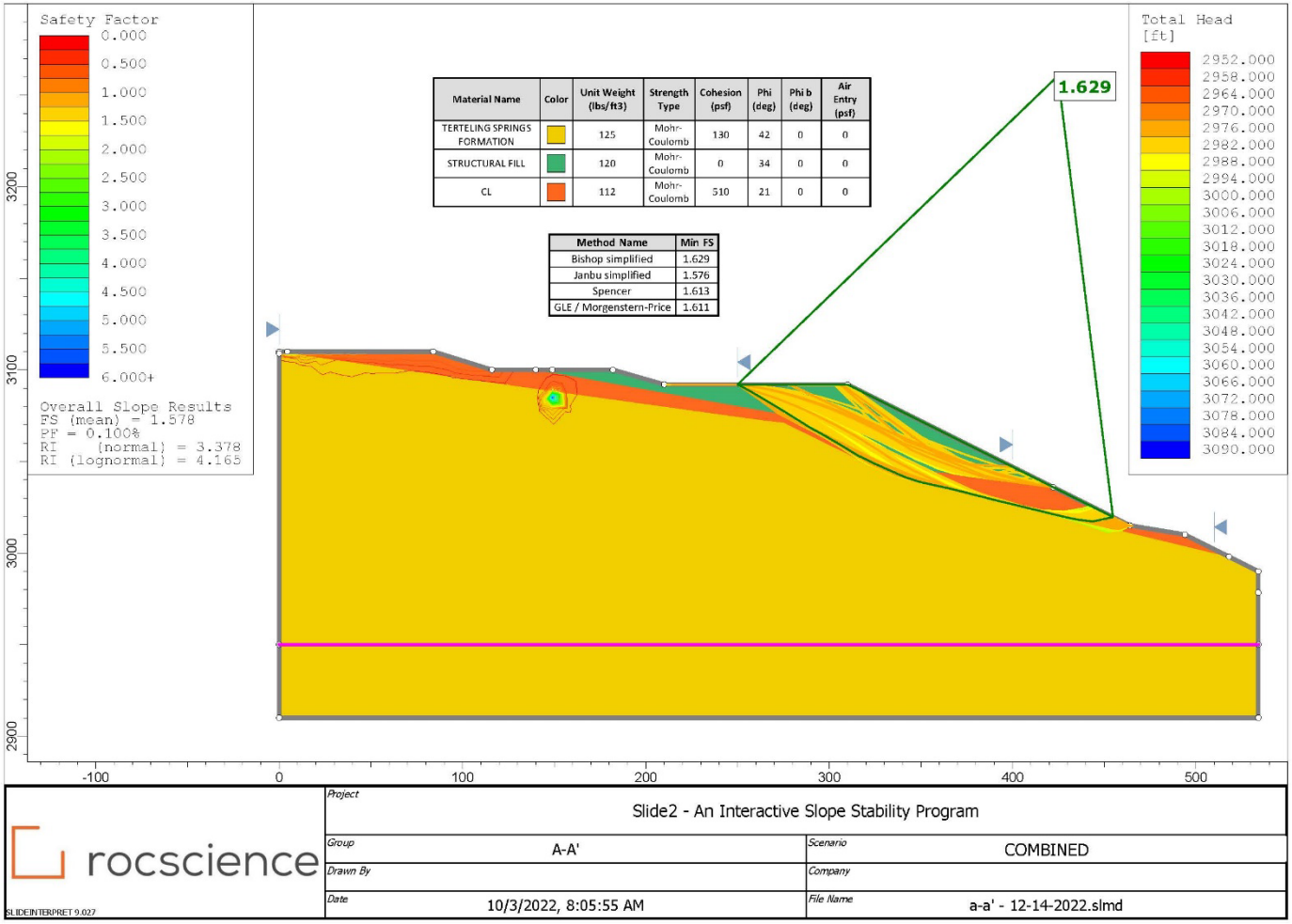

Figure B.1 Cross Section A-A' After Failure

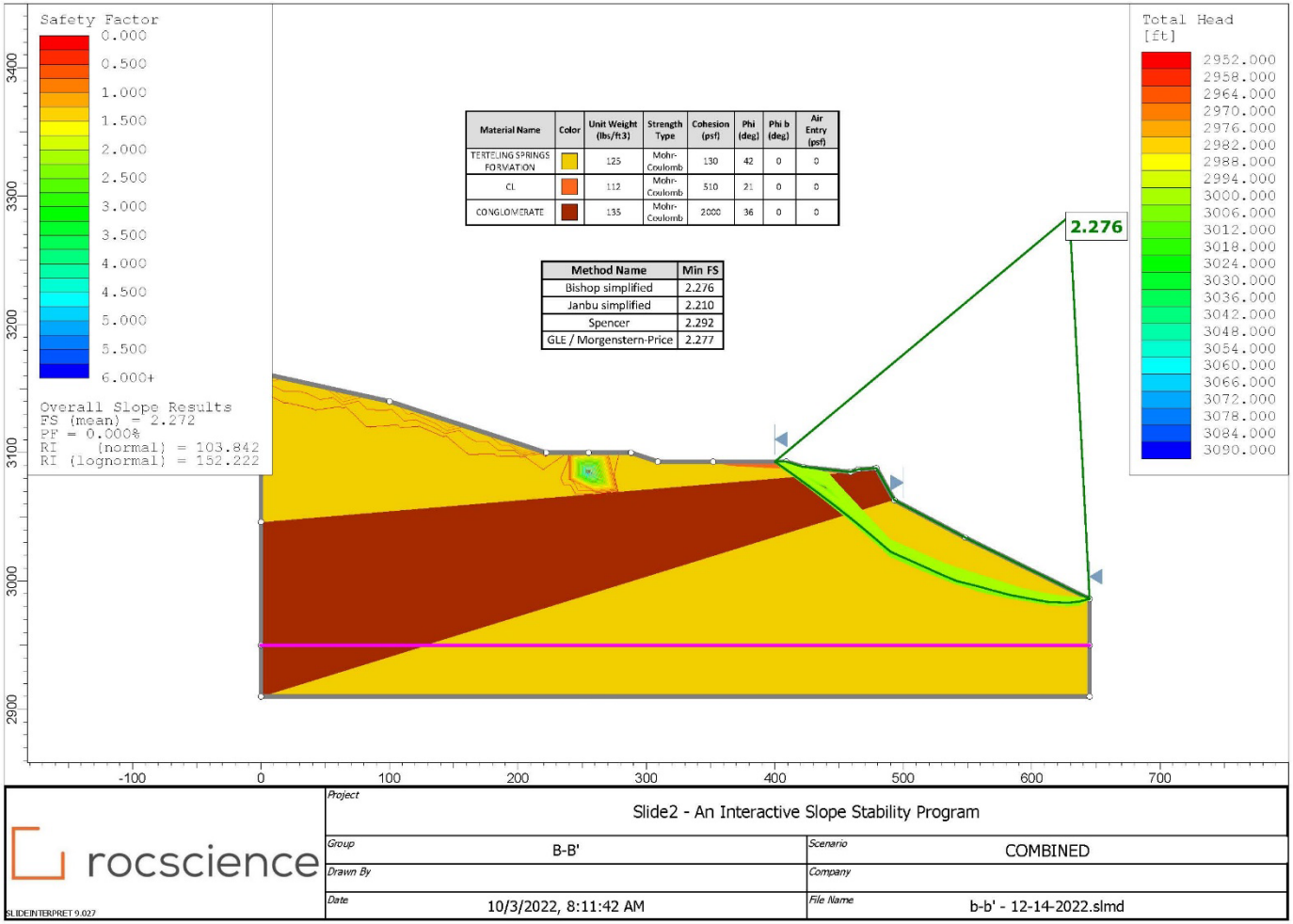

Figure B.2 Cross Section B-B' After Failure

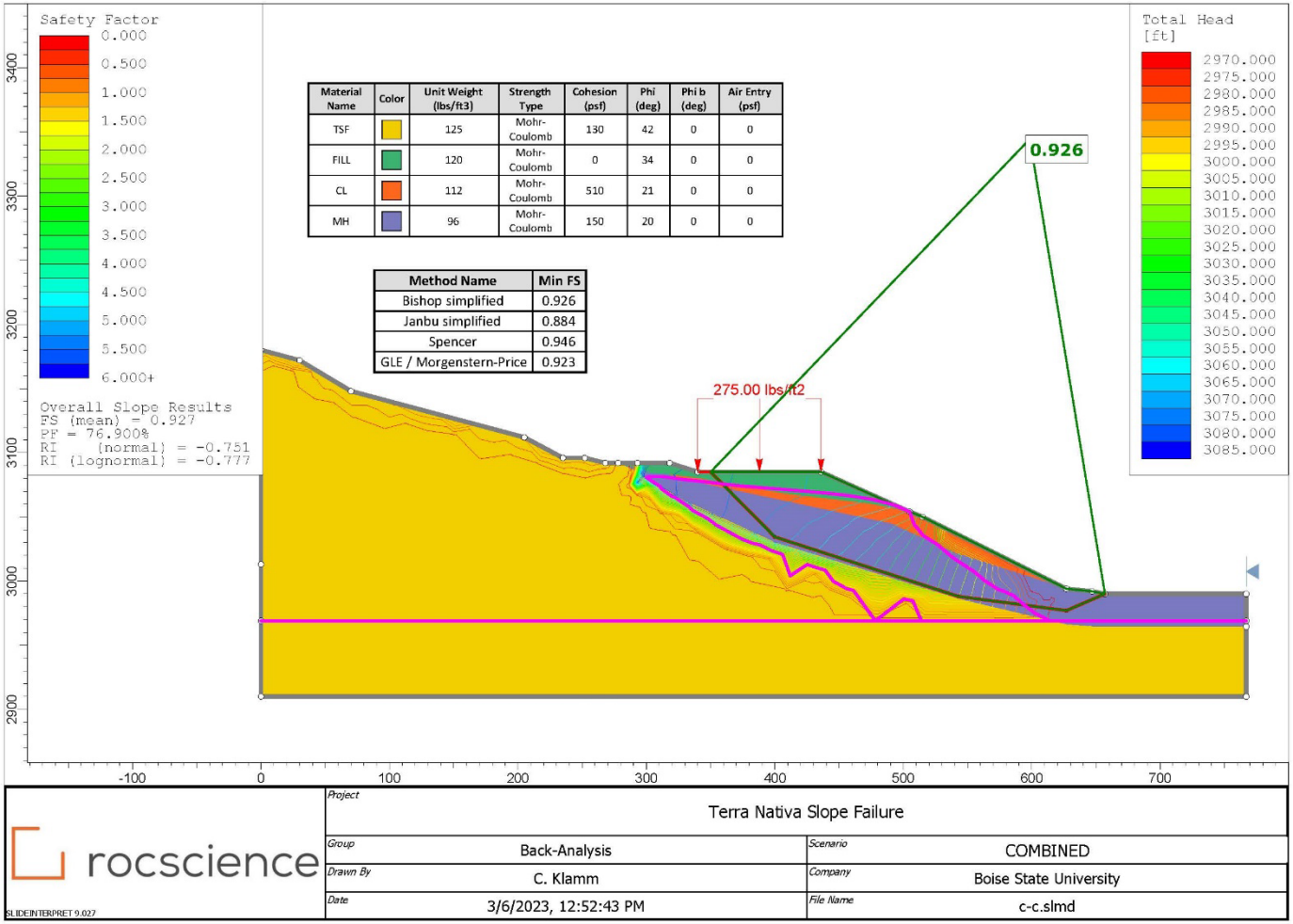

Figure B.3 Cross Section C-C' After Failure

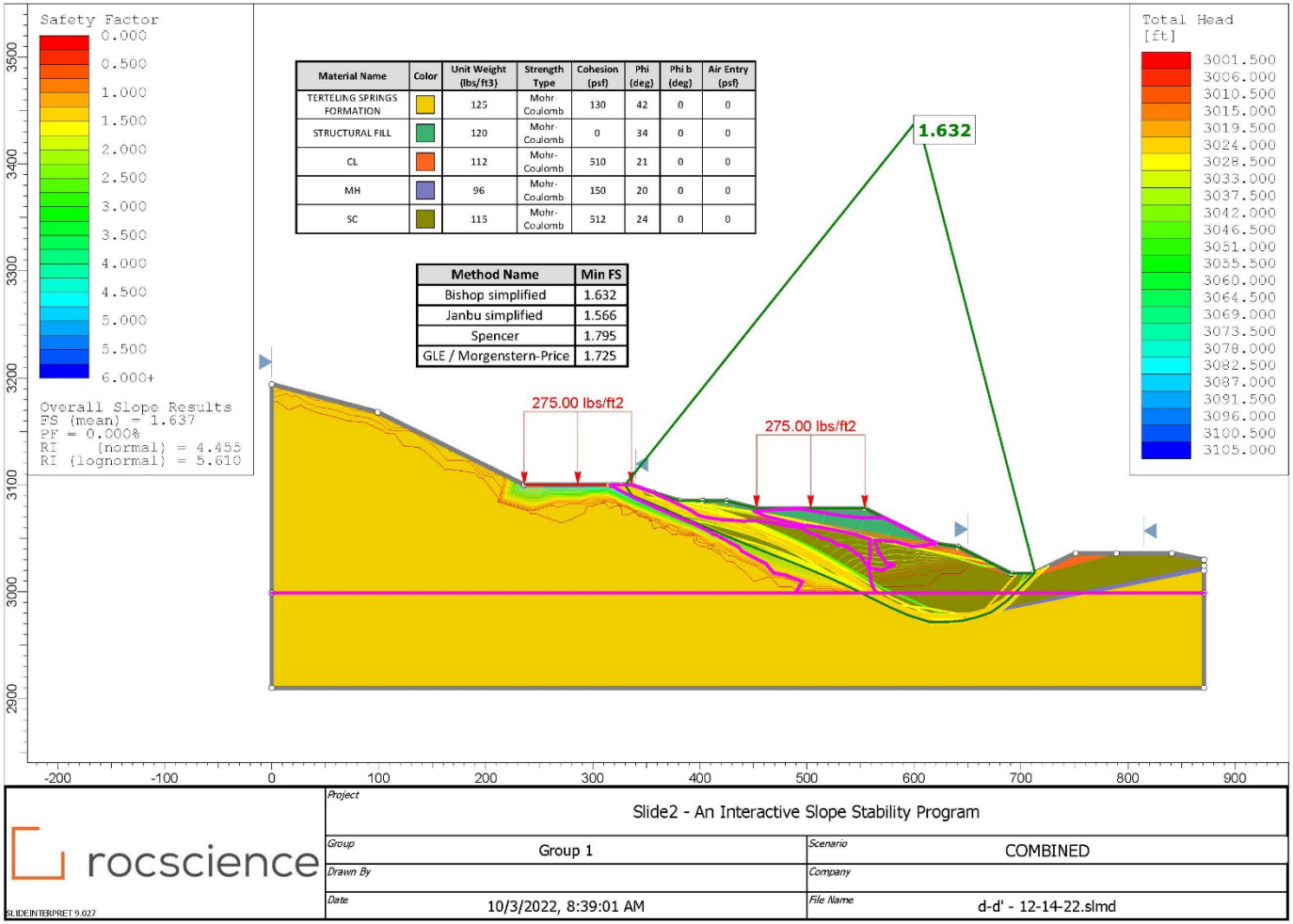

Figure B.4 Cross Section D-D' After Failure

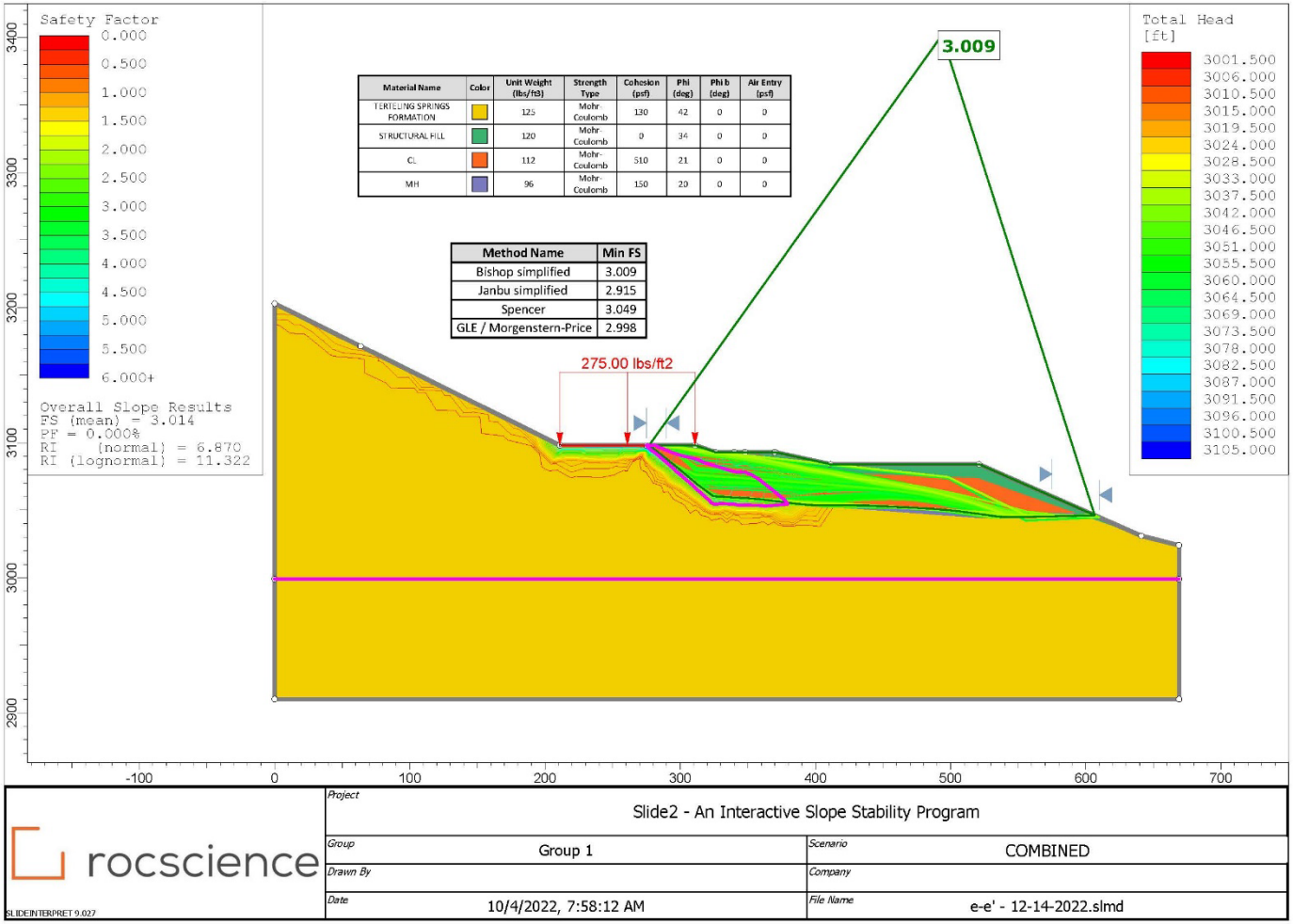

Figure B.5 Cross Section E-E' After Failure

APPENDIX C

Results of Slope Stability Analysis After Reinforcement

The following pages present cross sections C-C', D-D', and E-E' with their accompanying factors of safety after reinforcement with a 2'x2' reinforcement layout at the crest and toe.

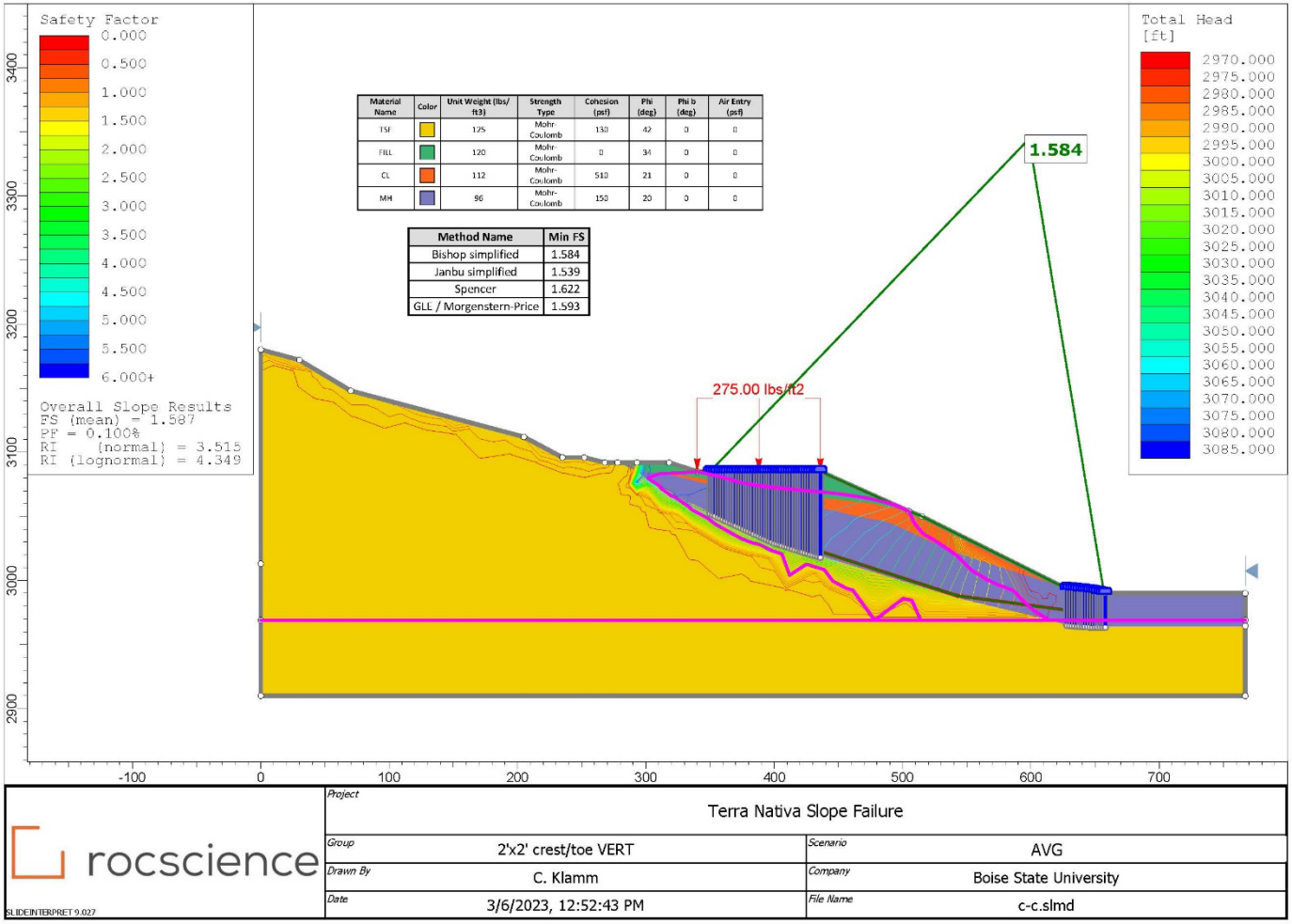

Figure C.1 Cross Section C-C' After Reinforcement

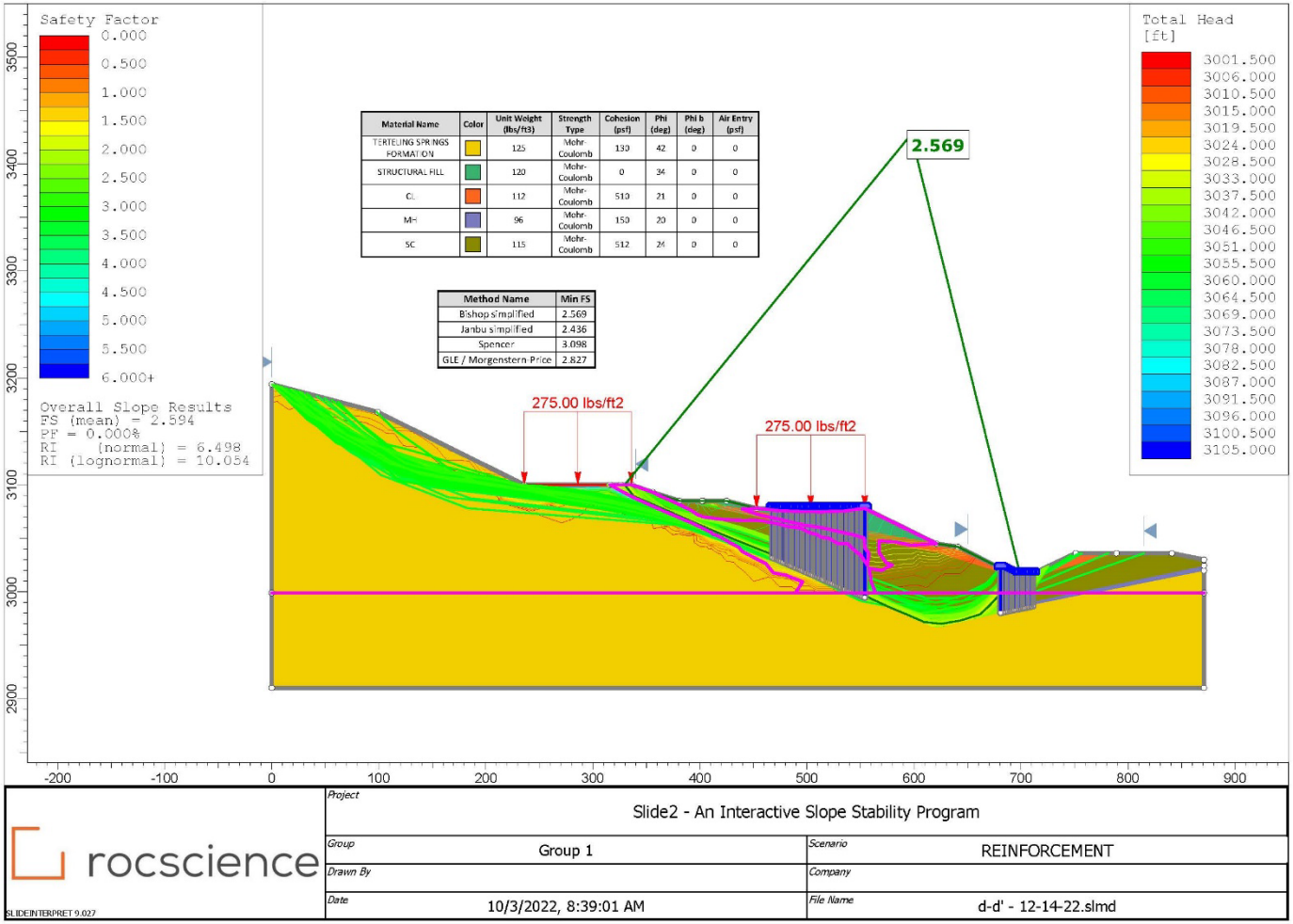

Figure C.2 Cross Section D-D' After Reinforcement

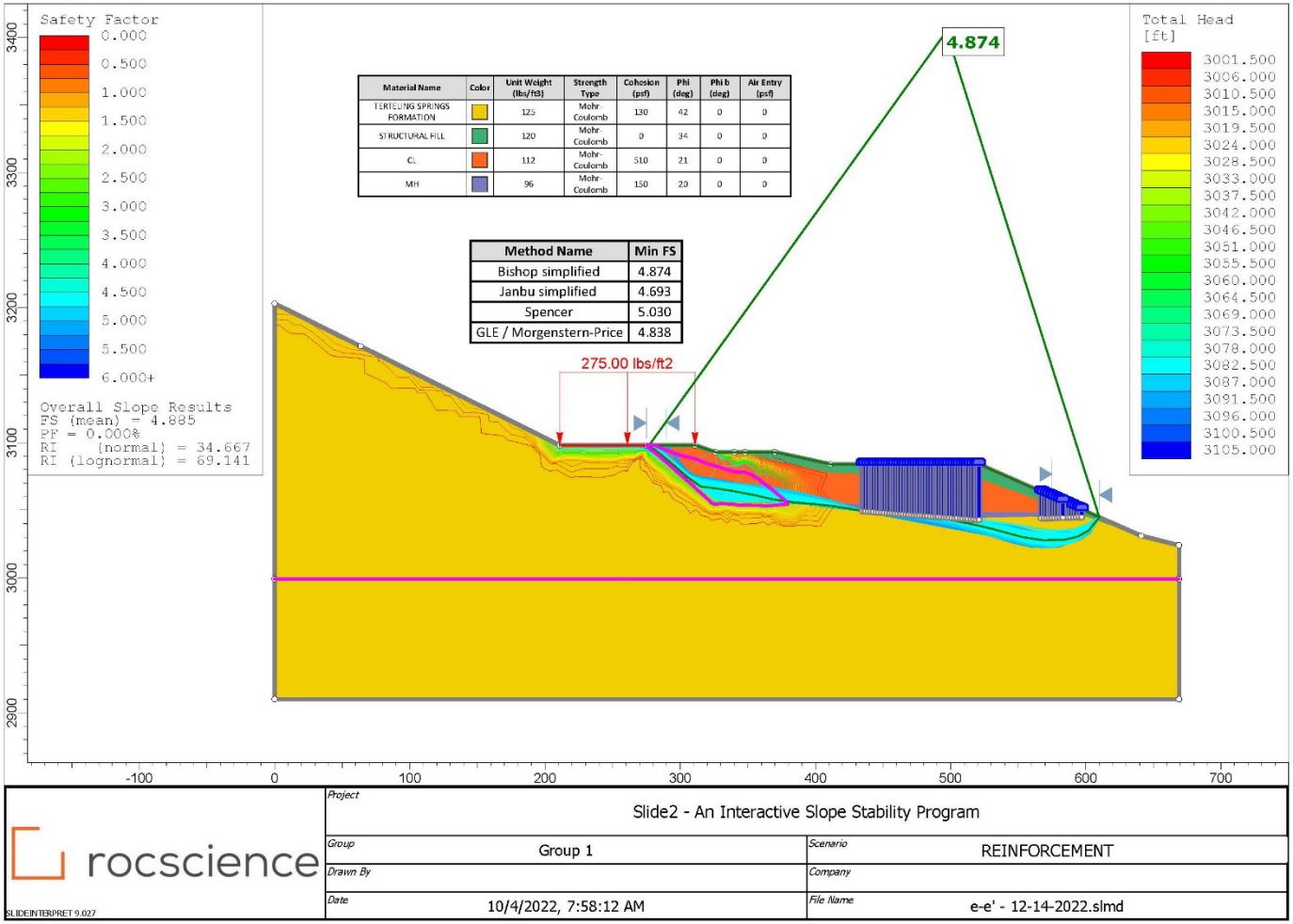

Figure C.3 Cross Section E-E' After Reinforcement